

Metal-insulator transition in the one-dimensional SU(N) Hubbard model

Roland Assaraf¹, Patrick Azaria², Michel Caffarel¹, and Philippe Lecheminant³

¹ CNRS-Laboratoire de Chimie Théorique, Université Pierre et Marie Curie, 4 Place Jussieu, 75252 Paris, France

² CNRS-Laboratoire de Physique Théorique des Liquides, Université Pierre et Marie Curie, 4 Place Jussieu, 75252 Paris, France

³ Laboratoire de Physique Théorique et Modélisation, Université de Cergy-Pontoise, Site de Saint Martin, 2 avenue Adolphe Chauvin, 95302 Cergy-Pontoise Cedex, France

(Received:)

We investigate the metal-insulator transition of the one-dimensional SU(N) Hubbard model for repulsive interaction. Using the bosonization approach a Mott transition in the charge sector at half-filling ($k_F = \pi/Na_0$) is conjectured for $N > 2$. Expressions for the charge and spin velocities as well as for the Luttinger liquid parameters and some correlation functions are given. The theoretical predictions are compared with numerical results obtained with an improved zero-temperature quantum Monte Carlo approach. The method used is a generalized Green's function Monte Carlo scheme in which the stochastic time evolution is partially integrated out. Very accurate results for the gaps, velocities, and Luttinger liquid parameters as a function of the Coulomb interaction U are given for the cases $N = 3$ and $N = 4$. Our results strongly support the existence of a Mott-Hubbard transition at a *non-zero* value of the Coulomb interaction. We find $U_c \sim 2.2$ for $N = 3$ and $U_c \sim 2.8$ for $N = 4$.

PACS No: 05.10.Ln, 71.10.Fd, 71.30.+h, 75.40.Gb

I. INTRODUCTION

Although the metal-insulator transition has certainly been one of the most studied phenomenon in condensed-matter physics, it is only in recent years that important progress has been achieved. This is mainly due to careful experimental and numerical studies but also to the improvement of the theoretical tools [1–3]. It has been proved extremely difficult to investigate the effect of strong correlations in dimensions greater than one, and it is only quite recently that, thanks to a new dynamical mean-field, our understanding has substantially progressed [4]. For one-dimensional systems, the situation is rather different: There exist powerful analytical and numerical approaches at our disposal. Moreover, from the experimental point of view, the Mott-transition can be realized in organic conductors [5] and quantum wires [6]. Therefore, one may expect to gain a lot of information on the physics of the metal-insulator transition.

In one dimension, it has been recognized very rapidly that umklapp processes are at the heart of the problem. In the Abelian bosonization formalism, one can draw a general and consistent picture of the Mott-transition. Indeed, the charge properties are expected to be described, in the absence of umklapp contributions, by a Luttinger liquid with only two independent parameters: The charge velocity u_c and the charge exponent K_c that controls the decay of correlation functions. These quantities, which are non-universal, completely characterize the low-energy properties of a one-dimensional system [7,8]. Within this framework, the effect of umklapp processes are investigated in perturbation theory, and one can write down an effective theory that describes the Mott-transition as well as a full description of the transport properties for

any commensurate filling [9,10]. The only parameter that controls the transition is the (in general unknown) Luttinger charge exponent K_c , and the transition is predicted to be universal of the Kosterlitz-Thouless (KT) type.

Most of the theoretical work in $d = 1$ focused on the properties of the standard SU(2) Hubbard model which, is known to be a Mott insulator at half-filling from its exact solution [11]. Some extension of this model was considered by introducing long-range hopping or finite-range interaction (nearest neighbor interaction for instance) [2]. In the present work, we study a most natural generalization of the usual Hubbard model: Instead of considering fermions with a two-valued spin index (with a SU(2) symmetry) we generalize to the case of an arbitrary SU(N) spin index. Apart from the theoretical interest it is important to emphasize that these additional degrees of freedom are realized physically through orbital degeneracy as for example in Mn oxides [3]. In this paper, we shall study the phase diagram of the one-dimensional SU(N) Hubbard model for repulsive interaction and at half filling corresponding to one “electron” per site. The Hamiltonian on a finite chain with L sites that we shall consider reads:

$$\mathcal{H} = -t \sum_{i=1}^L \sum_{a=1}^N \left(c_{ia}^\dagger c_{i+1a} + \text{H.c.} \right) + \frac{U}{2} \sum_{i=1}^L \left(\sum_{a=1}^N n_{ia} \right)^2 \quad (1)$$

where the fermion annihilation operator of spin index $a = 1, \dots, N$ at site i is denoted by c_{ia} and satisfies the canonical anticommutation relation:

$$\{c_{ia}, c_{jb}^\dagger\} = \delta_{ab} \delta_{ij}. \quad (2)$$

The density of species a at the i^{th} site is defined by: $n_{ia} = c_{ia}^\dagger c_{ia}$. In the following, we shall consider that the nearest-neighbor hopping (t) and the on-site interaction (U) are positive.

The Hamiltonian (1) is not exactly solvable by the Bethe ansatz for $N > 2$ and arbitrary U . It is however possible to solve the generalization of the Lieb-Wu Bethe ansatz equations for fermions carrying a $SU(N)$ spin index [12,13]. The result is that for any $N > 2$, there exists a Mott-Hubbard transition from a metallic phase to an antiferromagnetic insulating phase at a *finite* value of the coupling U . The transition is found to be of *first*-order in contrast with the accepted view that the metal-insulator transition in one-dimensional systems should be of the KT type. The point is that a projection onto the subspace of states having at most two electrons at each site is crucial for the use of the Bethe ansatz approach. The other configurations are automatically excluded by the Pauli principle in the $SU(2)$ Hubbard model whereas for $N > 2$ it is no longer the case. As a consequence, it is believed that the lattice model associated with the $SU(N)$ generalization of Lieb-Wu Bethe ansatz equations should coincide with an integrable *non-local* version of the $SU(N)$ Hubbard model (1) [12,13]. Although one naturally expects that the true $SU(N)$ Hubbard model will share some properties with its non-local partner, in particular the existence of a metallic phase at small enough U , the first-order character of the transition could take its origin in the nonlocality of the interaction. In any case, in order to study (1) one must abandon the exact Bethe ansatz approaches and resort to two powerful techniques available in one dimension: the bosonization and numerical approaches. As we shall show, none of these techniques is by itself sufficient to demonstrate the existence of the Mott transition. Regarding bosonization, the mere existence of the metal-insulator transition -even in the simplest scenario of a KT phase transition- relies on the knowledge of U dependence of the Luttinger parameter K_c , a nonuniversal quantity which can only be computed in a perturbative expansion in U . In other words, bosonization cannot tell us *whether* a given lattice model will undergo a Mott- U transition. However, it defines a rich theoretical framework in which many qualitative and quantitative predictions are obtained. This provides an essential guide for the numerical investigation of a particular lattice model. Regarding numerical investigations the situation is also not fully satisfactory. Beyond the evident problem of memory and CPU time limitations, it is well-known that it is very difficult to characterize a KT phase transition. As we shall emphasize later, it is almost impossible to discriminate between the opening of a charge gap at $U = 0$ and at a finite positive U , even when very accurate numerical data are at our disposal. The strategy employed in this work will consist in combining both approaches. Very strong evidences will be given in favor of a metal-insulator transition occurring at a finite positive value of the interaction U for $N > 2$.

Various numerical methods can be used to study the ground-state properties of Hamiltonian (1). In exact diagonalization methods [14] the exact ground-state eigenvector is calculated. Unfortunately, the rapid increase of the size of the Hilbert space restricts severely the attainable system sizes. In order to treat bigger systems two types of approach are at our disposal: The density matrix renormalization group (DMRG) method and the stochastic approaches.

Since its discovery a few years ago the DMRG method has been extensively used for studying various one-dimensional systems and coupled chain problems (for a review, see Ref. [15], for a detailed presentation of the method, see Refs. [16,17]). DMRG is a very efficient real-space numerical renormalization-group (RG) approach. The fundamental point which makes the method successful is the way that “important” degrees of freedom are chosen at each RG iteration. Instead of keeping the lowest eigenstates of the RG block considered as isolated from the outside world (as it was usually done in previous approaches), the states which are selected are the most probable eigenstates of the density matrix associated with the block considered as a part of the whole system. The main error of DMRG is related to the finite number of states kept at each iteration of the algorithm. In order to get the exact property the extrapolation to an infinite number of states has to be performed. At least for 1D and quasi-1D problems, and for systems having a small number of states per site, the errors obtained are small. Note also that DMRG works especially well when open boundary conditions are used. For periodic boundary conditions, errors are significantly larger.

In this paper we use an alternative approach based on a stochastic sampling of the configuration space. Such approaches are referred to as quantum Monte Carlo (QMC) methods. There exists a large variety of QMC approaches. A first set of methods is defined within a finite-temperature framework (Path-Integral Monte Carlo, World-line Monte Carlo, etc. . . , see e.g. Ref. [18]). In these approaches, the main systematic error is the high-temperature approximation associated with the Trotter break-up (Trotter or short-time error). When interested in obtaining the zero-temperature properties the number of “time slices” to consider must be taken large and the computational effort becomes important. Practical calculations have shown that the method is much less accurate than DMRG, at least for one-dimensional systems. In the second type of approaches used here, the stochastic sampling is directly defined within a zero-temperature framework. These methods are usually referred to as Green’s function Monte Carlo (GFMC) or projector Monte Carlo. For systems having a nodeless ground-state wave function as it is the case here, the GFMC method can be extremely powerful. The basic idea is to extract from a known trial wave function ψ_T its exact ground-state component ψ_0 . To do that an operator $G(\mathcal{H})$ acting as a filter is introduced. Statistical rules are defined in order to calculate stochastically the action

of the operator G on a given function. Apart from statistical fluctuations, the GFMC method is an exact method. It does not require an extrapolation to zero temperature as in finite-temperature schemes. In addition, there exists a so-called zero-variance property for the energy: The better the trial wave function ψ_T is, the smaller the statistical fluctuations are. In the limit of an exact wave function, the statistical fluctuations entirely disappear (zero-variance property). As an important consequence, by choosing a good enough trial wave function very accurate calculations can be performed (see, for example, Ref. [19]). Note that, in contrast with DMRG, the efficiency of GFMC does not depend on the specific type of boundary conditions chosen and that the number of states per site is not a critical parameter of the simulation. Here, it is an important point since the $SU(N)$ model displays 2^N states per site (for the $SU(4)$ case treated here it gives 16 states per site).

In order to improve further the accuracy of the approach we present a generalized version of the GFMC method in which the dynamics of the Monte Carlo process is partially integrated out. More precisely, we generalize an idea introduced by Trivedi and Ceperley in their GFMC study of the $S=1/2$ Heisenberg quantum antiferromagnet [19]. In the GFMC method the probability that the random walk remains a certain number of times in the same configuration is described by a Poisson distribution. It is then possible to sample the corresponding “trapping time” from this distribution and to weight the expectations values according to it. As remarked by Trivedi and Ceperley, doing this can lead to a considerable improvement in the simulation. This is particularly true when the wave function is localized (large U regime for our model, systems with deep potential wells, etc...). Here, we show that the method can be improved further by integrating out exactly the time evolution associated with this trapping phenomenon. Once this is done we are left with a random walk defined by an “escape transition probability” connecting non-identical configurations (the system never remains in the same configuration) and a modified branching term resulting from the time-integration. Note that introducing trapping times in averages helps a lot when optimizing the parameters of the trial wave function. Finally, we present an original method for computing the Luttinger liquid parameters within a QMC scheme. We show that these parameters can be obtained from a series of ground-state calculations of total energies of *real* -but not necessarily Hermitian- Hamiltonians. In this way we escape from the difficulty of calculating with QMC ground-state energies of the *complex* Hamiltonians resulting from the definition of the charge and spin stiffnesses. Although it is difficult to compare the efficiency of our generalized GFMC approach with DMRG (since the quality of GFMC simulations is too much dependent on the quality of the trial wave function used) we believe that the accuracy of our results is comparable or even better to what can be done with DMRG. In any case, our data are sufficiently ac-

curate to conclude to the existence of a metal-insulator phase transition in the model studied.

Very recently, Beccaria *et al.* [20] have proposed a QMC algorithm based on the use of Poisson processes. Their approach contains similar ideas. However, in contrast with the present approach no importance sampling is used and no integration of the Poisson dynamics is performed. It should also be noted that the use of Poisson processes for describing the time evolution of systems trapped in some configuration is not restricted to quantum systems. Krauth and collaborators have proposed related ideas within the context of classical Monte Carlo simulations [21,22].

The organization of the paper is as follows. In section II, a bosonization approach of the $SU(N)$ Hubbard model will be given. Some of the results has already been obtained by Affleck [23] whereas additional new ones will also be useful to compare with the numerical simulations. The purpose of section III is to give a presentation of the GFMC method together with our generalization based on the partial integration of the dynamics. The practical implementations of the GFMC approach for the Hamiltonian (1) will be discussed in section IV and the numerical results for $N = 2, 3, 4$ will be presented in section V. Finally, section VI gives a summary of the work together with a comparison between the physical results obtained for the $SU(N)$ Hubbard model and those corresponding to its nonlocal integrable version. In the Appendix we give some details of computation occurring in section II.

II. THE $SU(N)$ HUBBARD MODEL

In this section, we shall use a bosonization approach (for recent reviews see Refs. [8,24]) to study the $SU(N)$ Hubbard model. Before doing that, let us first discuss the symmetries of the model.

The Hamiltonian (1) has a $U(1) \otimes SU(N)$ symmetry:

$$\begin{aligned} c_{ia} &\rightarrow e^{i\theta} c_{ia} \\ c_{ia} &\rightarrow U_{ab} c_{ib} \end{aligned} \quad (3)$$

where the matrix U belongs to $SU(N)$. These symmetries express the conservation of the charge and spin invariance under a $SU(N)$ rotation. The associated generators are given by the following operators:

$$\begin{aligned} \mathcal{N} &= \sum_{i,a} n_{ia} \\ \mathcal{S}^A &= \sum_i \mathcal{S}_i^A \end{aligned} \quad (4)$$

with

$$\mathcal{S}_i^A = c_{ia}^\dagger \mathcal{T}_{ab}^A c_{ib} \quad (5)$$

where the summation over repeated indexes (except for lattice indexes) is assumed in the following. In the latter

equation, the $N^2 - 1$ matrices \mathcal{T}^A are the generators of the Lie algebra of $SU(N)$ in the fundamental representation. They satisfy the commutation relation:

$$[\mathcal{T}^A, \mathcal{T}^B] = if^{ABC}\mathcal{T}^C, \quad (6)$$

f^{ABC} being the structure constants of the Lie algebra and the generators are normalized according to $\text{Tr}(\mathcal{T}^A\mathcal{T}^B) = \delta^{AB}/2$. The conservation law associated with the $U(1)$ symmetry allows to study the Hamiltonian (1) for a fixed density n . The Coulomb interaction can thus be rewritten, up to a constant, in terms of the $SU(N)$ spin operator:

$$\frac{U}{2} \left(\sum_{a=1}^N n_{ia} \right)^2 = -\frac{UN}{N+1} \mathcal{S}_i^A \mathcal{S}_i^A \quad (7)$$

where we have used the identity:

$$\mathcal{T}_{ab}^A \mathcal{T}_{de}^A = \frac{1}{2} \left(\delta_{ae} \delta_{bd} - \frac{1}{N} \delta_{ab} \delta_{de} \right). \quad (8)$$

The relation (7) makes explicit the $SU(N)$ invariance of the model.

The Hamiltonian (1) is not exactly solvable by the Bethe ansatz for $N > 2$ and arbitrary U , even if, as already emphasized, some integrable non-local extension of (1) with a $SU(N)$ symmetry can be considered. The situation is simpler in the limit $U \rightarrow \infty$ and at half filling (one ‘‘electron’’ per site), i.e. when $k_F = \pi/Na_0$ (a_0 being the lattice spacing). In that case, it can be shown that (1) reduces to the $SU(N)$ Heisenberg anti-ferromagnetic chain for which an exact solution is available. As shown by Sutherland [25], this latter model is critical with $N - 1$ massless bosonic modes with the same velocity. In the Conformal Field Theory (CFT) language, the central charge of the model in the infrared (IR) limit is $c = N - 1$ and using a non-Abelian bosonization of (1), Affleck [23] identifies the nature of the critical theory in the spin sector as the $SU(N)_1$ Wess-Zumino-Novikov-Witten (WZNW) model. In the following, we shall present both non-Abelian and Abelian bosonization approaches of the $SU(N)$ Hubbard model (1) at half filling and give a number of results that will be essential for discussing the numerical data presented in section V.

A. Continuum limit

In the continuum limit, the spectrum around the two Fermi points $\pm k_F$ is linearized and gives rise to left-moving fermions ψ_{aL} and right-moving fermions ψ_{aR} . In this low-energy procedure, the lattice fermion operators c_{ia} are expressed in terms of these left-right moving fermions as:

$$\frac{c_{ia}}{\sqrt{a_0}} \rightarrow \psi_a(x) \sim \psi_{aR}(x) e^{ik_F x} + \psi_{aL}(x) e^{-ik_F x}, \quad (9)$$

where $x = ia_0$. In this continuum limit, the non-interacting part of the Hamiltonian (1) corresponds to the Hamiltonian density of N free relativistic fermions:

$$\mathcal{H}_0 = -iv_F \left(: \psi_{aR}^\dagger \partial_x \psi_{aR} : - : \psi_{aL}^\dagger \partial_x \psi_{aL} : \right) \quad (10)$$

where the normal ordering $::$ with respect of the Fermi sea is assumed and the Fermi velocity v_F is given by:

$$v_F = 2ta_0 \sin \frac{\pi}{N}. \quad (11)$$

In the continuum limit, the $SU(N)$ spin operator (5) decomposes into an uniform and a $2k_F$ contribution:

$$\frac{\mathcal{S}_i^A}{a_0} \rightarrow \mathcal{S}^A(x) \simeq \mathcal{J}^A(x) + (e^{2ik_F x} \mathcal{N}^A(x) + \text{H.c.}) \quad (12)$$

where the $2k_F$ contribution is given by:

$$\mathcal{N}^A = \psi_{aL}^\dagger \mathcal{T}_{ab}^A \psi_{bR} \quad (13)$$

whereas the uniform part reads: $\mathcal{J}^A = \mathcal{J}_R^A + \mathcal{J}_L^A$ with

$$\mathcal{J}_{R(L)}^A = : \psi_{aR(L)}^\dagger \mathcal{T}_{ab}^A \psi_{bR(L)} : \quad (14)$$

These left-right $SU(N)$ spin currents obey the following Operator Product Expansion (OPE) (see the Appendix):

$$\lim_{x \rightarrow y} \mathcal{J}_{R(L)}^A(x) \mathcal{J}_{R(L)}^B(y) \sim \frac{-\delta^{AB}}{8\pi^2(x-y)^2} \mp \frac{f^{ABC}}{2\pi(x-y)} \mathcal{J}_{R(L)}^C(y) \quad (15)$$

which shows that they satisfy the $SU(N)_1$ Kac-Moody (KM) algebra [24,26]. In the same way, the total charge density $\sum_a n_{ia}$ reads in the continuum limit:

$$\sum_a n_{ia} \rightarrow a_0^{1/2} \left(\mathcal{J}^0(x) + \left(e^{-2ik_F x} \psi_{aR}^\dagger(x) \psi_{aL}(x) + \text{H.c.} \right) \right) \quad (16)$$

where $\mathcal{J}^0 = \mathcal{J}_R^0 + \mathcal{J}_L^0$ and

$$\mathcal{J}_{R(L)}^0 = : \psi_{aR(L)}^\dagger \psi_{aR(L)} : \quad (17)$$

are the $U(1)$ right and left charge currents. These currents satisfy the OPE:

$$\lim_{x \rightarrow y} \mathcal{J}_{R(L)}^0(x) \mathcal{J}_{R(L)}^0(y) \sim -\frac{N}{4\pi^2(x-y)^2} \quad (18)$$

and $\mathcal{J}_{R(L)}^0$ belongs to the $U(1)_N$ KM algebra.

With these identifications, it is not difficult to show (see the Appendix) that the free part of the Hamiltonian (10) can be expressed only in terms of spin and charge currents (the so-called Sugawara form):

$$\mathcal{H}_0 = \mathcal{H}_{0s} + \mathcal{H}_{0c} \quad (19)$$

with

$$\mathcal{H}_{0s} = \frac{2\pi v_F}{N+1} (: \mathcal{J}_R^A \mathcal{J}_R^A : + : \mathcal{J}_L^A \mathcal{J}_L^A :) \quad (20)$$

and

$$\mathcal{H}_{0c} = \frac{\pi v_F}{N} (: \mathcal{J}_R^0 \mathcal{J}_R^0 : + : \mathcal{J}_L^0 \mathcal{J}_L^0 :). \quad (21)$$

At the level of the free theory, spin and charge degrees of freedom decouple. The symmetry of the free Hamiltonian \mathcal{H}_0 in the continuum limit is therefore enlarged to give: $U(1)_L \otimes SU(N)_L \otimes U(1)_R \otimes SU(N)_R$. The Hamiltonian \mathcal{H}_{0s} is nothing but the Sugawara form of the $SU(N)_1$ WZNW model [24,26]. It is a conformally invariant theory with central charge $c = N - 1$ ($N - 1$ massless bosons). The contribution \mathcal{H}_{0c} describes the $U(1)$ charge degrees of freedom and has central charge $c = 1$ (1 massless boson).

The non-trivial part of the problem stems from the Coulomb interaction (7). At sufficiently small $U \ll t$, from Eq. (7), we see that its contribution will be given by the OPE:

$$\mathcal{V}(x) = -U a_0 \frac{N}{N+1} \lim_{\epsilon \rightarrow 0} \mathcal{S}^A(x+\epsilon) \mathcal{S}^A(x). \quad (22)$$

From Eq. (12), there are three contributions to \mathcal{V} :

$$\mathcal{V} = \mathcal{V}_0 + \mathcal{V}_{2k_F} + \mathcal{V}_{4k_F}. \quad (23)$$

The first term is the uniform $k = 0$ component while the others contain oscillating factors $e^{\pm 2ik_F x}$ and $e^{\pm 4ik_F x}$. Neglecting all oscillatory contributions, we are thus left with the uniform part \mathcal{V}_0 . Performing the necessary OPEs (see the Appendix), one finds that the total effective low energy Hamiltonian density separates into two commuting charge and spin parts:

$$\mathcal{H} = \mathcal{H}_c + \mathcal{H}_s \quad (24)$$

with

$$\mathcal{H}_c = \frac{\pi v_c}{N} (: \mathcal{J}_R^0 \mathcal{J}_R^0 : + : \mathcal{J}_L^0 \mathcal{J}_L^0 :) + G_c \mathcal{J}_R^0 \mathcal{J}_L^0 \quad (25)$$

and

$$\mathcal{H}_s = \frac{2\pi v_s}{N+1} (: \mathcal{J}_R^A \mathcal{J}_R^A : + : \mathcal{J}_L^A \mathcal{J}_L^A :) + G_s \mathcal{J}_R^A \mathcal{J}_L^A \quad (26)$$

where the renormalized velocities are:

$$\begin{aligned} v_s &= v_F - \frac{U a_0}{2\pi} \\ v_c &= v_F + (N-1) \frac{U a_0}{2\pi} \end{aligned} \quad (27)$$

and the current-current couplings in the charge and the spin sectors are given by:

$$\begin{aligned} G_c &= \frac{N-1}{N} U a_0 \\ G_s &= -2U a_0. \end{aligned} \quad (28)$$

Apart from a velocity renormalization, the effect of the Coulomb interaction is exhausted in the two marginal interactions in both charge and spin sectors. When $U > 0$, the spin current-current interaction is marginal irrelevant. At the IR fixed point, $G_s^* = 0$, the Hamiltonian in the spin sector is that of the $SU(N)_1$ WZNW model. On the other hand, the current-current interaction in the charge sector is exactly marginal since one can diagonalize \mathcal{H}_c with a Bogolioubov transformation to recover the Tomonaga-Luttinger Hamiltonian. Therefore, \mathcal{H}_c describes the line of fixed points of the Luttinger liquid.

From the above analysis we conclude that the $SU(N)$ Hubbard model at half filling is massless for small $U > 0$. The spin sector is described by the $SU(N)_1$ WZNW model while the charge sector is a Luttinger liquid with continuously varying exponents. The main point in the above analysis is the absence of umklapp terms which, when $N = 2$, opens a gap in the charge sector for an infinitesimal value of the interaction. At this point it is worth recalling that the main approximation made in the above analysis is the omission of the oscillating contributions \mathcal{V}_{2k_F} and \mathcal{V}_{4k_F} . This is a reasonable assumption as far as U is not too large. However one expects, on general grounds, that umklapp processes should contribute at sufficiently large U and that a Mott transition to an insulating phase should occur at a finite U_c . Indeed, in the $U \rightarrow \infty$ limit, we have an insulating phase where the spin degrees of freedom are described by the $SU(N)$ Heisenberg antiferromagnet. We shall return to this point later. For now let us concentrate on the properties of the metallic phase.

B. The metallic phase

At this point, we introduce N chiral bosonic fields $\phi_{aR(L)}$, $a = (1, \dots, N)$, using the Abelian bosonization of Dirac fermions [24]:

$$\psi_{aR(L)} = \frac{\kappa_a}{\sqrt{2\pi}} : \exp(\pm i\sqrt{4\pi}\phi_{aR(L)}) : \quad (29)$$

where the bosonic fields satisfy the following commutation relation $[\phi_{aR}, \phi_{bL}] = \frac{i}{4}\delta_{ab}$. The anticommutation between fermions with different spin indexes is realized through the presence of Klein factors (here Majorana fermions) κ_a with the following anticommutation rule: $\{\kappa_a, \kappa_b\} = 2\delta_{ab}$. As in the $N = 2$ case, it is suitable to switch to a basis where the charge and spin degrees of freedom single out. To this end, let us introduce a charge bosonic field $\Phi_{cR(L)}$ and $N - 1$ spin bosonic fields $\Phi_{msR(L)}$, $m = (1, \dots, N - 1)$ as follows:

$$\begin{aligned} \Phi_{cR(L)} &= \frac{1}{\sqrt{N}} (\phi_1 + \dots + \phi_N)_{R(L)} \\ \Phi_{msR(L)} &= \frac{1}{\sqrt{m(m+1)}} (\phi_1 + \dots + \phi_m - m\phi_{m+1})_{R(L)}. \end{aligned} \quad (30)$$

The transformation (30) is canonical and preserves the bosonic commutation relations. The inverse transformation is easily found to be:

$$\begin{aligned}\phi_{1R(L)} &= \frac{1}{\sqrt{N}}\Phi_{cR(L)} + \sum_{l=1}^{N-1} \frac{\Phi_{lsR(L)}}{\sqrt{l(l+1)}} \\ \phi_{aR(L)} &= \frac{1}{\sqrt{N}}\Phi_{cR(L)} - \sqrt{\frac{a-1}{a}}\Phi_{(a-1)sR(L)} \\ &\quad + \sum_{l=a}^{N-1} \frac{\Phi_{lsR(L)}}{\sqrt{l(l+1)}}, \quad a = 2, \dots, N-1 \\ \phi_{NR(L)} &= \frac{1}{\sqrt{N}}\Phi_{cR(L)} - \sqrt{\frac{N-1}{N}}\Phi_{(N-1)sR(L)}.\end{aligned}\quad (31)$$

In this new basis, the Hamiltonian density in the spin sector at the $SU(N)_1$ fixed point reads:

$$\mathcal{H}_s^* = \frac{u_s}{2} \sum_{m=1}^{N-1} \left(:(\partial_x \Phi_{ms})^2: + :(\partial_x \Theta_{ms})^2: \right) \quad (32)$$

where u_s is the spin velocity at the fixed point and

$$\begin{aligned}\Phi_{ms} &= \Phi_{msL} + \Phi_{msR} \\ \Theta_{ms} &= \Phi_{msL} - \Phi_{msR}.\end{aligned}\quad (33)$$

This representation makes clear the fact that the central charge in the spin sector is indeed $c = N - 1$.

Let us now concentrate on the charge sector. It is not difficult to show, using Eqs. (17, 29) and (30) that the charge current expresses as:

$$\mathcal{J}_{R(L)}^0 = \sqrt{\frac{N}{\pi}} \partial_x \Phi_{cR(L)}. \quad (34)$$

Therefore, the Hamiltonian density (25) in the charge sector reads:

$$\begin{aligned}\mathcal{H}_c &= \frac{v_c}{2} \left(:(\partial_x \Phi_c)^2: + :(\partial_x \Theta_c)^2: \right) \\ &\quad + (N-1) \frac{Ua_0}{\pi} \partial_x \Phi_{cL} \partial_x \Phi_{cR}\end{aligned}\quad (35)$$

where we have introduced the total charge bosonic field: $\Phi_c = \Phi_{cR} + \Phi_{cL}$ and its dual: $\Theta_c = \Phi_{cL} - \Phi_{cR}$. The Hamiltonian (35) can be written in the Luttinger liquid form:

$$\mathcal{H}_c = \frac{u_c}{2} \left(\frac{1}{K_c} :(\partial_x \Phi_c)^2: + K_c :(\partial_x \Theta_c)^2: \right) \quad (36)$$

where the charge exponent K_c and the renormalized charge velocity u_c are given by:

$$\begin{aligned}K_c &= \frac{1}{\sqrt{1 + (N-1)Ua_0/\pi v_F}} \\ u_c &= v_F \sqrt{1 + (N-1)Ua_0/\pi v_F}.\end{aligned}\quad (37)$$

The U dependence of the Luttinger parameters K_c and u_c given in the above expressions should not be taken too seriously. Indeed, the continuum limit approach is strictly speaking valid only provided $U/t \ll 1$. In this regime one has

$$\begin{aligned}K_c &\sim 1 - (N-1) \frac{Ua_0}{2\pi v_F} \\ u_c &\sim v_F + (N-1) \frac{Ua_0}{2\pi}.\end{aligned}\quad (38)$$

The physically relevant question is now what happens for higher values of the interaction U . In the absence of umklapp terms, the accepted view is that the effect of interaction corresponds to a renormalization of the Luttinger parameters K_c and u_c as well as the spin velocity u_s which have therefore to be thought as phenomenological parameters as the Landau coefficients in the Fermi liquid theory [7,8]. These parameters completely characterize the low energy properties of the metallic phase as we shall see now. Let us first discuss the electronic Green's function defined by:

$$G_{ab}(x, \tau) = \langle \psi_a^\dagger(x, \tau) \psi_b(0, 0) \rangle, \quad (39)$$

τ being the imaginary time. This correlation function can be computed using Eqs. (9, 29) and (31). After some calculations, one finds:

$$\begin{aligned}G_{ab}(x, \tau) &\sim \frac{\delta_{ab}}{2\pi} \left[\frac{1}{x^2 + u_c^2 \tau^2} \right]^{\alpha/2} \\ &\quad \times \left[\frac{\exp(ik_F x)}{(ix + u_c \tau)^{1/N} (ix + u_s \tau)^{1-1/N}} \right. \\ &\quad \left. + \frac{\exp(-ik_F x)}{(-ix + u_c \tau)^{1/N} (-ix + u_s \tau)^{1-1/N}} \right]\end{aligned}\quad (40)$$

where the exponent α is given by:

$$\alpha = \frac{1}{2NK_c} (1 - K_c)^2. \quad (41)$$

This allows to give an estimate of the single particle density of states which is related to the electronic Green's function at $x = 0$:

$$\rho(\omega) \sim |\omega|^\alpha. \quad (42)$$

Similarly, K_c determines the singularity of the momentum distribution $n_a(k)$ around the Fermi point k_F :

$$n_a(k) = n_a(k_F) + \text{Cte} \operatorname{sgn}(k - k_F) |k - k_F|^\alpha \quad (43)$$

and the momentum distribution function has a power law singularity at the Fermi level unlike a standard Fermi liquid. This anomalous power law behavior for any finite value of N is inherent of a Luttinger liquid.

The computation of the $SU(N)$ spin-spin correlation function:

$$\Delta^{AB}(x, \tau) = \langle \mathcal{S}^A(x, \tau) \mathcal{S}^B(0, 0) \rangle \quad (44)$$

is more involved. It can be shown that the leading asymptotics of this correlation function is given by the $2k_F$ part:

$$\Delta^{AB}(x, \tau) \sim \delta^{AB} \frac{\cos(2k_F x)}{(x^2 + u_c^2 \tau^2)^{K_c/N} (x^2 + u_s^2 \tau^2)^{1-1/N}}. \quad (45)$$

We deduce from the above correlation function the low temperature dependence of the NMR relaxation rate T_1 :

$$\frac{1}{T_1 T} \sim T^{2/N+2K_c/N-2}. \quad (46)$$

As seen, once the U dependence of the Luttinger parameters u_c , K_c and u_s is known, the low energy properties of the metallic phase are entirely determined. These parameters are non-universal and cannot be obtained for arbitrary U by the continuum limit approach. Although $K_c < 1$ when $U > 0$, one does not know its minimum value. It is only in the $N = 2$ case, that the Luttinger parameters can be extracted from the exact solution [27–29]. When $N > 2$ no exact solution is available and one has to use numerical computations to estimate these parameters. This will be done for the two cases $N = 3$ and $N = 4$ in section V. Before doing that, let us discuss about the Mott transition that should occur in the problem for a finite critical value of the repulsion U for $N > 2$.

C. The Mott transition

The very difference between the $N = 2$ and $N > 2$ cases lies in the fact that there is no umklapp term at half filling in the bare Hamiltonian in the continuum limit. The reason for this is that these terms came with oscillating factors and were omitted for small value of the repulsion. However, in the RG strategy one has to look at the stability of the Luttinger fixed line and any operator that is compatible with the symmetry of the problem should be taken into account: they will be generated during the renormalization process. In our problem, the important symmetries are the $SU(N)$ spin rotation invariance, chiral invariance and translation invariance.

From Eqs. (9, 29) and (30), one easily finds that under a translation by one lattice site, the charge field Φ_c is shifted according to:

$$\Phi_c \rightarrow \Phi_c + \sqrt{\frac{\pi}{N}}. \quad (47)$$

Therefore one can add any operator in the charge sector that is invariant under the transformation (47) and will be necessary generated by higher order in perturbation theory. The operator with the smallest scaling dimension that is invariant under (47) is:

$$\mathcal{H}_{umklapp} = -G_u : \cos\left(\sqrt{4\pi N}\Phi_c\right) :. \quad (48)$$

Other operators, with higher scaling dimensions, that couple spin and charge degrees of freedom may also be included. This is the reason why one cannot exclude the possibility of a charge density wave (CDW) instability. For instance, such processes are present in the extended $SU(2)$ Hubbard model at half filling [30]. Although it requires some formal proof, we expect that, due to the fact that in the present model the interaction is local in the density, the leading umklapp contribution should only affect the charge sector. We have checked that this is indeed true for the particular cases, $N = 3$ and $N = 4$ [31]. We have shown indeed by perturbation theory that the oscillating contributions \mathcal{V}_{2k_F} and \mathcal{V}_{4k_F} generate $6k_F$ and $4k_F$ processes for $N = 3$ and $N = 4$ respectively. Up to irrelevant operators, the only contribution we found is precisely (48) with $N = 3$ and $N = 4$. In any case in what follows, we shall thus make the hypothesis, first made by Affleck [23], that all the effects of high energy processes are exhausted by (48) for the general $SU(N)$ case. Consequently, the effective Hamiltonian density in the spin sector is still given by the $SU(N)_1$ WZNW model and the effective Hamiltonian in the charge sector is now:

$$\mathcal{H}_c = \frac{u_c}{2} \left(\frac{1}{K_c} : (\partial_x \Phi_c)^2 : + K_c : (\partial_x \Theta_c)^2 : \right) - G_u : \cos\left(\sqrt{4\pi N}\Phi_c\right) :. \quad (49)$$

Rescaling the fields as $\Phi_c \rightarrow \Phi_c \sqrt{K_c}$ and $\Theta_c \rightarrow \Theta_c / \sqrt{K_c}$, the Hamiltonian (49) in the charge sector becomes the Hamiltonian of the sine-Gordon model:

$$\mathcal{H}_c = \frac{u_c}{2} \left(: (\partial_x \Phi_c)^2 : + : (\partial_x \Theta_c)^2 : \right) - G_u : \cos\left(\sqrt{4\pi N K_c} \Phi_c\right) :. \quad (50)$$

Since the scaling dimension of the cosine term in (50) is $\Delta_u = N K_c$, we deduce that a gap opens in the charge sector when:

$$K_c = \frac{2}{N}. \quad (51)$$

On the other hand, when $K_c < 2/N$, the umklapp term is irrelevant and the system remains in the metallic phase described in the preceding subsection. Therefore, as U increases, K_c will decrease from 1 at $U = 0$ to $K_c = 2/N$ at a critical value of the interaction U_c where a Mott transition to an insulating phase occurs. Within this scheme, the phase transition is expected to be of the KT type. Of course when $U > U_c$, K_c vanishes so that the jump is $1 - 2/N$ and is universal. The present approach cannot give an accurate value of U_c . However, one can get a rough estimate of U_c using Eqs. (11, 37) and (51):

$$\frac{U_c}{t} = \frac{\pi}{2} \frac{N^2 - 4}{N - 1} \sin \frac{\pi}{N}. \quad (52)$$

In the insulating phase, the charge field Φ_c is locked in a special well of the sine-Gordon model (50) and the leading asymptotics of the $SU(N)$ spin-spin correlation functions is now:

$$\Delta^{AB}(x, \tau) \sim \lambda_1 \delta^{AB} \frac{\cos(2k_F x)}{(x^2 + u_s^2 \tau^2)^{1-1/N}} \quad (53)$$

where λ_1 is a non-universal constant stemming from the charge degrees of freedom. One recovers the result previously derived by Affleck [23]. The NMR relaxation rate behaves now as $1/(T_1 T) \sim T^{2/N-2}$. Finally, let us note that there are other harmonics $4k_F, 6k_F, \dots$ in the $SU(N)$ spin density (12) that will be generated by higher orders in perturbation theory. Together with the uniform contribution with scaling dimension 1, these terms will give subleading power law contributions in the $SU(N)$ spin-spin correlation function (53). These operators correspond to the primary fields of $SU(N)_1$ WZNW transforming to other representation of $SU(N)$ than the fundamental one. One should recall that for the $SU(N)_1$ WZNW, there are $N-1$ primary fields [26]. A primary field $\tilde{\phi}_a$ ($a = 1, \dots, N-1$) of $SU(N)_1$ transforms according to the a^{th} basic representation of $SU(N)$ (Young tableau with a boxes and a single column) and has scaling dimension: $\Delta_a = a(N-a)/N$. We thus expect the following asymptotics for Δ^{AB} with some non-universal constants (λ_a):

$$\Delta^{AB}(x, \tau) \sim -\frac{\delta^{AB}}{8\pi^2} \left(\frac{1}{(u_s \tau - ix)^2} + \frac{1}{(u_s \tau + ix)^2} \right) + \delta^{AB} \sum_{a=1}^{N-1} \lambda_a \frac{\cos(2ak_F x)}{(x^2 + u_s^2 \tau^2)^{a-a^2/N}} \quad (54)$$

up to logarithmic contributions originating from the marginal irrelevant current-current interaction in the spin sector [32].

We end this subsection by giving the low-temperature expression of the uniform susceptibility χ and the specific heat of the $SU(N)$ Hubbard model in the insulating antiferromagnetic phase. The continuum density that describes the behavior of the $SU(N)$ spins degrees of freedom in a uniform magnetic field H is given by:

$$\mathcal{H}_H = \frac{u_s}{2} \sum_{m=1}^{N-1} \left(:(\partial_x \Phi_{ms})^2 : + :(\partial_x \Theta_{ms})^2 : \right) - H \sum_{m=1}^{N-1} \mathcal{J}^m \quad (55)$$

where we have neglected the marginally irrelevant current-current interaction. In Eq. (55), we have considered a uniform magnetic field along the diagonal \mathcal{T}^m , ($m = 1, \dots, N-1$) generators of $SU(N)$ that span the Cartan subalgebra of $SU(N)$. According to our normalization convention, they can be written in $N \times N$ diagonal matrices as follows:

$$\mathcal{T}^m = \frac{1}{\sqrt{2m(m+1)}} \text{diag}(1, 1, \dots, -m, 0, \dots, 0) \quad (56)$$

with $m = 1, \dots, N-1$ and $-m$ is located on the $m+1$ element of the diagonal. Using the bosonization correspondence (29) and the canonical transformation (31), the total density Hamiltonian (55) in a magnetic field can be written as:

$$\mathcal{H}_H = \frac{u_s}{2} \sum_{m=1}^{N-1} \left(:(\partial_x \Phi_{ms})^2 : + :(\partial_x \Theta_{ms})^2 : \right) - \frac{H}{\sqrt{2\pi}} \sum_{m=1}^{N-1} \partial_x \Phi_{ms}. \quad (57)$$

Doing the substitution:

$$\partial_x \Phi_{ms} \rightarrow \partial_x \Phi_{ms} + \frac{H}{\sqrt{2\pi} u_s}, \quad (58)$$

we obtain the expression of the uniform susceptibility of the $SU(N)$ Heisenberg antiferromagnet:

$$\chi = \frac{N-1}{2\pi u_s} \quad (59)$$

which is nothing but $N-1$ times the uniform susceptibility of the $SU(2)$ Heisenberg antiferromagnet. This result is easy to understand since the critical theory in the spin sector corresponds to $N-1$ decoupled massless bosonic modes. Finally, using the general formula of the specific heat at low temperatures for a conformally invariant theory [33], one has for the $SU(N)$ Heisenberg antiferromagnet:

$$C_V = \frac{\pi(N-1)}{3u_s} T. \quad (60)$$

Before closing this section, it is important to emphasize that the Mott transition expected in the bosonization approach relies on the full expression of $K_c(U)$ as function of the interaction. However, one should stress that this parameter cannot be obtained for arbitrary U within this approach and only in the weak coupling limit $U \ll t$ where the model is in its metallic phase. To conclude in favour of the existence of a Mott transition for a finite value of the Coulomb interaction, one has thus to compute $K_c(U)$ of the lattice model by an independent approach. Since the $SU(N)$ Hubbard model with $N > 2$ is not exactly soluble, one cannot determine the expression $K_c(U)$ by the Bethe ansatz as for the standard Hubbard model [27–29]. We shall thus compute the value $K_c(U)$ of the lattice model using very accurate numerical calculations based on QMC methods described in the next section. In section V, we shall then compare the numerical results with the predictions of the bosonization approach given in this section to conclude on the existence of a Mott transition in the model.

III. THE NUMERICAL APPROACH

In this section we present our improved zero-temperature Green's function Monte Carlo method used for computing ground-state properties. In the first part a sketchy but self-contained presentation of the basic GFMC method is given. In addition to introducing our notations for the next part, this section will enable the interested reader to understand all the practical aspects of the method. The second part is devoted to the presentation of the generalized GFMC method itself.

A. Green's function Monte Carlo

As already noticed in the introduction the basic idea of the GFMC method is to extract from a known trial wave function $|\psi_T\rangle$ the exact ground-state component $|\psi_0\rangle$. To do that an operator $G(\mathcal{H})$ acting as a filter is introduced. For continuum problems standard choices are $G(\mathcal{H}) = \exp(-\tau\mathcal{H})$ (Diffusion Monte Carlo) or $G(\mathcal{H}) = 1/(1 + \tau(E - \mathcal{H}))$ (Green's function Monte Carlo). For a lattice problem or any model with a finite number of states (finite matrix) a natural choice to consider is

$$G(\mathcal{H}) \equiv 1 - \tau(\mathcal{H} - E_T) \quad (61)$$

where τ plays the role of a time-step (a positive constant) and E_T is some reference energy. If τ is chosen sufficiently small and $|\psi_T\rangle$ has a non-zero overlap with the ground-state, the exact ground-state is filtered out as follows

$$\lim_{P \rightarrow \infty} G(\mathcal{H})^P |\psi_T\rangle \sim |\psi_0\rangle. \quad (62)$$

This result is easily obtained by expanding $|\psi_T\rangle$ within the complete set of eigenstates of \mathcal{H} .

In Monte Carlo schemes, successive applications of the operator $G(\mathcal{H})$ on $|\psi_T\rangle$ are done using probabilistic rules. These rules are implemented in configuration space where the trial wave function and matrix elements of \mathcal{H} are easily evaluated. In what follows we shall denote by $|i\rangle$ an arbitrary configuration of the system. To give an example, in actual calculations presented below we consider $|i\rangle = |i^{(1)}\rangle \dots |i^{(N)}\rangle$ with $|i^{(a)}\rangle \equiv |n_{1a}, \dots, n_{La}\rangle$ where L is the number of sites, a the SU(N) color index, and n_{ia} the occupation number of site i ($n_{ia} = 0$ or 1) for the species a .

In this work Hamiltonians considered are of the form:

$$\mathcal{H} = T + V \quad (63)$$

where T is the kinetic term (a non-diagonal operator) and V is a (diagonal) potential term. For fermions in one dimension it is known that by choosing a suitable labelling of the sites, matrix elements of the kinetic term can all be made negative

$$\langle i|T|j\rangle < 0 \quad (i \neq j). \quad (64)$$

A most important consequence of this property is that the exact ground-state has a constant sign. In other words, simulations presented here are free of the sign problem.

Let us now introduce the following transition probability

$$P_{i \rightarrow j}(\tau) = \psi_T(j) \langle j | [1 - \tau(\mathcal{H} - E_L)] | i \rangle \frac{1}{\psi_T(i)} \quad (65)$$

where $\psi_T(i)$ are the components of the vector $|\psi_T\rangle$, $\psi_T(i) \equiv \langle i | \psi_T \rangle$, and E_L is a diagonal operator called the local energy and defined as follows

$$\langle i | E_L | j \rangle = \delta_{ij} E_L(i)$$

with

$$E_L(i) = \frac{\langle i | \mathcal{H} | \psi_T \rangle}{\langle i | \psi_T \rangle}. \quad (66)$$

Note the important relation associated with the definition of the local energy:

$$(\mathcal{H} - E_L) | \psi_T \rangle = 0. \quad (67)$$

To define a transition probability $P_{i \rightarrow j}$ must fulfill the two following conditions. First, the sum over final states, $\sum_j P_{i \rightarrow j}$, must be equal to one. Here, this is true as a direct consequence of (67). Second, $P_{i \rightarrow j}$ must be positive. To see this and for later use, let us distinguish between the cases $i = j$ and $i \neq j$.

For $i = j$ we have

$$P_{i \rightarrow i}(\tau) = 1 + \tau T_L(i) \quad (68)$$

where $T_L(i) \equiv E_L(i) - H_{ii}$. Using (63), $T_L(i)$ can be rewritten as

$$T_L(i) = \frac{\langle i | T | \psi_T \rangle}{\langle i | \psi_T \rangle}, \quad (69)$$

$T_L(i)$ is called the local kinetic energy. Because of (64) it is a negative quantity and the transition probability can be made positive by taking τ sufficiently small. More precisely, the time-step must verify

$$0 < \tau < \text{Min}_i[-1/T_L(i)]. \quad (70)$$

Note that the upper bound is a non-zero quantity for a finite system.

On the other hand, when $i \neq j$ we have

$$P_{i \rightarrow j}(\tau) = -\tau H_{ij} \frac{\psi_T(j)}{\psi_T(i)} \quad (i \neq j), \quad (71)$$

a positive expression since $\psi_T(i)$ is chosen to be positive and off-diagonal terms H_{ij} are negative (Eq. (64)).

Using expressions (68) and (71) for the transition probability random walks in configuration space can be generated. By averaging over configurations, statistical estimates for various quantities can be defined. A first

important example is the calculation of the variational energy associated with $|\psi_T\rangle$ (variational Monte Carlo). The variational energy is defined as

$$E_v(\psi_T) = \frac{\langle \psi_T | \mathcal{H} | \psi_T \rangle}{\langle \psi_T | \psi_T \rangle}. \quad (72)$$

Here, it is rewritten as

$$E_v(\psi_T) = \lim_{K \rightarrow \infty} \frac{1}{K} \sum_{i=1}^K E_L(i) = \langle\langle E_L \rangle\rangle_{(P)} \quad (73)$$

where $\langle\langle \dots \rangle\rangle_{(P)}$ is the stochastic average over configurations $|i\rangle$ generated using the transition probability P , K being the number of configurations calculated. Equation (73) holds because $\psi_T(i)^2$ is the stationary density of the stochastic process, that is

$$\sum_i \psi_T(i)^2 P_{i \rightarrow j}(\tau) = \psi_T(j)^2 \quad \forall j. \quad (74)$$

This property is directly verified by using expressions (65) and (67).

As already pointed out, the estimate of the exact energy is based on the stochastic calculation of $[1 - \tau(\mathcal{H} - E_T)]^n |\psi_T\rangle$, Eq. (62). Introducing between each operator in the product the decomposition of the identity over the basis set, $1 = \sum_i |i\rangle\langle i|$, and making use of the definition of the transition probability, (65), we get the following path integral representation

$$\begin{aligned} [1 - \tau(\mathcal{H} - E_T)]^P |\psi_T\rangle &= \sum_{i_0 \dots i_P} \psi_T(i_0)^2 \prod_{k=0}^{P-1} P_{i_k \rightarrow i_{k+1}} \\ &\prod_{k=0}^{P-1} w_{i_k i_{k+1}} \frac{1}{\psi_T(i_P)} |i_P\rangle \end{aligned} \quad (75)$$

where the weights w_{ij} are defined as follows

$$w_{ij} \equiv \frac{\langle i | [1 - \tau(\mathcal{H} - E_T)] | j \rangle}{\langle i | [1 - \tau(\mathcal{H} - E_L)] | j \rangle} \quad (76)$$

or more explicitly,

$$\begin{aligned} w_{ij} &= 1 \quad i \neq j, \\ w_{ii} &= \frac{1 - \tau(H_{ii} - E_T)}{1 - \tau(H_{ii} - E_L(i))} \quad i = j. \end{aligned} \quad (77)$$

From (62) the exact energy can be obtained as

$$E_0 = \lim_{P \rightarrow \infty} \frac{\langle \psi_T | \mathcal{H} [1 - \tau(\mathcal{H} - E_T)]^P | \psi_T \rangle}{\langle \psi_T | [1 - \tau(\mathcal{H} - E_T)]^P | \psi_T \rangle} \quad (78)$$

which is rewritten here in terms of stochastic averages as

$$E_0 = \lim_{P \rightarrow \infty}$$

$$\langle\langle E_L(i_P) \prod_{k=0}^{P-1} w_{i_k i_{k+1}} \rangle\rangle_{(P)} / \langle\langle \prod_{k=0}^{P-1} w_{i_k i_{k+1}} \rangle\rangle_{(P)}. \quad (79)$$

In order to compute the averages appearing in that expression two strategies can be employed. First, formula (79) can be directly used as it stands: Paths are generated using the transition probability and the local energy at each step is weighted by the quantity $W = \prod_k w_{i_k i_{k+1}}$. This approach where the number of configurations is kept fixed and the weights are carried out along trajectories is usually referred to as the Pure Diffusion or Green's function Monte Carlo method. For extended systems such as those considered here, this approach is not optimal. Indeed, it is important to sample less frequently regions of configuration space where the total weight is small and to accumulate statistics where it is large. To realize this, a birth-death process (or branching process) associated with the local weight is introduced. In practice, it consists in adding to the standard stochastic move defined by the transition probability, a new step in which the current configuration is destroyed or copied a number of times proportional to the local weight. Denoting m_{ij} the number of copies (multiplicity) of the state j , we take

$$m_{ij} \equiv \text{int}(w_{ij} + \eta) \quad (80)$$

where $\text{int}(x)$ denotes the integer part of x , and η a uniform random number on $(0, 1)$. Adding a branching process can be viewed as sampling with a generalized transition probability $P_{i \rightarrow j}^*(\tau)$ defined as

$$\begin{aligned} P_{i \rightarrow j}^*(\tau) &\equiv P_{i \rightarrow j}(\tau) w_{ij} \\ &= \psi_T(j) \langle j | [1 - \tau(\mathcal{H} - E_T)] | i \rangle \frac{1}{\psi_T(i)}. \end{aligned} \quad (81)$$

Of course, the normalization is not constant (the population fluctuates) and P^* is not a genuine transition probability. However, we can still define a stationary density for it. From Eq. (81) we see that the stationary condition is obtained when E_T is chosen to be the exact energy E_0 , and that the density is $\psi_T(i) \psi_0(i)$. Accordingly, by using a stabilized population of configurations the exact energy may be now obtained as

$$E_0 = \langle\langle E_L \rangle\rangle_{(P,w)}. \quad (82)$$

Note the use of an additional subscript w in the average to recall the presence of the branching process.

At this point, we shall not expand further the method. For more details regarding the implementation of GFMC to lattice systems the interested reader is referred to Refs. [34,35,19,36]. Let us just emphasize on two important aspects. First, there exists a so-called zero-variance property for the energy: The better the trial wave function ψ_T is, the smaller the statistical fluctuations are. In the limit of an exact wave function for which the local energy is a constant, fluctuations entirely disappear (zero

variance). From this important remark follows that in any QMC method, it is crucial to optimize as much as possible the trial wave function used. Of course, in practice, a compromise between the complexity of the wave function and the gain in reduction of variance has to be found.

Once a good trial wave function has been chosen, the only room left for improvement is the implementation of the dynamical process itself. In the algorithm presented here the only dynamical parameter which can be adjusted is the time-step τ . In a configuration $|i\rangle$ associated with a small local kinetic energy $T_L(i)$, the system remains in this configuration a relatively large time and a large value of τ is necessary to help the system to escape from it. Unfortunately, because of the constraint (68) ($P_{i\rightarrow i}$ must be positive) configurations with a high local kinetic energy impose a small value of τ . In order to circumvent this difficulty, we propose to integrate out exactly the time evolution of the system when trapped in a given configuration. This idea is developed in the next section.

B. GFMC and Poisson processes

Consider the probability that the system remains in a given configuration i a number of times equal to n . It is given by

$$P_i(n) \equiv P(i_1 = i, \tau; \dots; i_n = i, \tau; i_{n+1} \neq i, \tau) = [P_{i\rightarrow i}(\tau)]^n [1 - P_{i\rightarrow i}(\tau)] \quad (83)$$

$P_i(n)$ defines a normalized discrete Poisson distribution. In terms of the local kinetic energy it can be rewritten as

$$P_i(n) = -\tau T_L(i) \exp[n \ln(1 + \tau T_L(i))] \quad (84)$$

where the integer n runs from zero to infinity. To describe transitions towards states j different from i we introduce the following escape transition probability

$$\tilde{P}_{i\rightarrow j} = \frac{P_{i\rightarrow j}(\tau)}{1 - P_{i\rightarrow i}(\tau)} \quad j \neq i. \quad (85)$$

Using Eqs. (68) and (69) $\tilde{P}_{i\rightarrow j}$ is rewritten in the most explicit form

$$\tilde{P}_{i\rightarrow j} = \frac{H_{ij}\psi_T(j)}{\sum_{k \neq i} H_{ik}\psi_T(k)} \quad j \neq i. \quad (86)$$

Note that this transition probability is positive, normalized, and independent of the time-step τ . Now, by using both probabilities, $P_i(n)$ and $\tilde{P}_{i\rightarrow j}$, the path integral representation of $G(\mathcal{H})^P |\psi_T\rangle$, formula (75), can be rewritten as

$$[1 - \tau(\mathcal{H} - E_T)]^P |\psi_T\rangle = \sum_{(i,n) \in \mathcal{C}_P} \psi_T(i_0)^2$$

$$\left[\prod_{k=0}^{l-1} \mathcal{P}_{i_k}(n_k) \tilde{P}_{i_k \rightarrow i_{k+1}} \right] \mathcal{P}_{i_l}(n_l) \prod_{k=0}^l w_{i_k}^{n_k} \frac{1}{\psi_T(i_l)} |i_l\rangle \quad (87)$$

where the sum is performed over the set of all families of states $(i_0 \dots i_l)$ with multiplicities $(n_0 \dots n_l)$ verifying $\sum_{k=0}^{l-1} (n_k + 1) + n_l = P$. In a given family successive states are different and the variable n_k represents the number of times the system remains in configuration i_k . The set of all families is denoted \mathcal{C}_P and an arbitrary element is written $(i, n) \equiv (i_0 \dots i_l, n_0 \dots n_l)$. Since off-diagonal weights are equal to one, Eq. (77), a shortened notation for the diagonal weights, $w_i \equiv w_{ii}$, has been introduced.

Now, let us remark that the time-step τ plays a role in the path integral formula (87) only when the system is trapped into a given configuration. Indeed, both the escape probability \tilde{P} and the off-diagonal weight w_{ij} are independent of τ . As an important consequence the limit $\tau \rightarrow 0$ and $P \rightarrow \infty$ with $P\tau = t$ can be done exactly. In this limit the discrete Poisson process $\mathcal{P}_i(n)$ defined in (84) converges to a continuous Poissonian distribution for the variable $\theta = n\tau$

$$\mathcal{P}_i(\theta) = \frac{1}{\bar{\theta}_i} e^{-\theta/\bar{\theta}_i}. \quad (88)$$

In this formula $\bar{\theta}_i$ represents the average time spent in configuration i . In what follows we shall refer to it as the average trapping time, its expression is

$$\bar{\theta}_i = -1/T_L(i). \quad (89)$$

The fact that $\bar{\theta}_i$ is inversely proportional to the local kinetic energy is explained as follows. When the kinetic energy is small the system is almost blocked in its configuration and $\bar{\theta}$ is large. In contrast, when a large kinetic energy is available, the system can escape easily from its current configuration and $\bar{\theta}$ is small. As already remarked the escape transition probability is independent of τ and is therefore not affected by the zero-time-step limit. Finally, after exponentiating the product of weights, the path integral can be rewritten in the form

$$e^{-t(\mathcal{H} - E_T)} |\psi_T\rangle = \sum_{i_0 \dots i_l} \int_0^{+\infty} d\theta_0 \dots \int_0^{+\infty} d\theta_l \psi_T(i_0)^2$$

$$\left[\prod_{k=0}^{l-1} \mathcal{P}_{i_k}(\theta_k) \tilde{P}_{i_k \rightarrow i_{k+1}} \right] \mathcal{P}_{i_l}(\theta_l) e^{-\sum_{k=0}^l \theta_k (E_L(i_k) - E_T)} \frac{1}{\psi_T(i_l)} |i_l\rangle \quad (90)$$

with the constraint that the trapping times verify $\sum_{k=0}^l \theta_k = t$.

In order to compute ground-state properties the limit $t \rightarrow \infty$ must be performed, Eq. (62). In this limit the constraint $\sum_{k=0}^l \theta_k = t$ can be relaxed and, quite remarkably, integrations over the Poisson distributions for the different trapping times can be performed. For large enough time t we obtain

$$e^{-t(\mathcal{H} - E_T)} |\psi_T\rangle \sim_{l \rightarrow \infty}$$

$$\sum_{i_0 \dots i_l} \psi_T(i_0)^2 \prod_{k=0}^{l-1} \tilde{P}_{i_k \rightarrow i_{k+1}} \prod_{k=0}^l \tilde{w}_{i_k} \frac{-1}{T_L(i_l)} \frac{1}{\psi_T(i_l)} |i_l\rangle \quad (91)$$

where the new integrated weights \tilde{w} are found to be

$$\tilde{w}_i = \frac{T_L(i)}{E_T - H_{ii}}. \quad (92)$$

In the same way as before the exact energy can be obtained as

$$E_0 = \lim_{t \rightarrow \infty} \frac{\langle \psi_T | \mathcal{H} e^{-t(\mathcal{H} - E_T)} | \psi_T \rangle}{\langle \psi_T | e^{-t(\mathcal{H} - E_T)} | \psi_T \rangle}. \quad (93)$$

In terms of stochastic averages it gives

$$E_0 = \lim_{l \rightarrow \infty} \frac{\langle \langle E_L(i_l) \bar{\theta}_{i_l} \prod_{k=0}^l \tilde{w}_{i_k} \rangle \rangle_{(\tilde{P})}}{\langle \langle \bar{\theta}_{i_l} \prod_{k=0}^l \tilde{w}_{i_k} \rangle \rangle_{(\tilde{P})}}. \quad (94)$$

where configurations are generated using the escape transition probability \tilde{P} .

As in the standard approach it is preferable to simulate the weights via a branching process. Here also, the reference energy E_T stabilizing the population is given by the exact energy, E_0 . The new stationary density writes

$$\pi(i) \sim \psi_T(i) \psi_0(i) / \bar{\theta}_i \quad (95)$$

up to an immaterial normalization constant. Finally, our estimator for E_0 is

$$E_0 = \frac{\langle \langle \bar{\theta}_i E_L(i) \rangle \rangle_{(\tilde{P}, \tilde{w})}}{\langle \langle \bar{\theta}_i \rangle \rangle_{(\tilde{P}, \tilde{w})}} \quad (96)$$

where configurations are generated using \tilde{P} and branched with \tilde{w} . Note that the variational energy can be recovered by removing the branching process ($\tilde{w} = 1$)

$$E_v(\psi_T) = \frac{\langle \langle \bar{\theta}_i E_L(i) \rangle \rangle_{(\tilde{P})}}{\langle \langle \bar{\theta}_i \rangle \rangle_{(\tilde{P})}} \quad (97)$$

IV. COMPUTATIONAL DETAILS

In this section some important aspects of the practical implementation of the GFMC approach to the SU(N) Hubbard model are presented.

A. Hard-core boson Hamiltonian

The Hamiltonian considered here is the one-dimensional SU(N) Hubbard model described by (1). Simulations are performed for a finite ring of length L . In one dimension the sites can be labelled in such way that the hopping term connects only sites represented by consecutive integers. As a consequence no fermion sign appears, except eventually when a fermion crosses the boundary ($1 \rightarrow L$ or $L \rightarrow 1$). By choosing either periodic or antiperiodic boundary conditions this sign can always be absorbed and our model (1) becomes equivalent to a model made up with hard-core bosons and described by

$$\mathcal{H} = -t \sum_{i=1}^L \sum_{a=1}^N c_{i+1a}^+ c_{ia} + \text{H.c.} + \frac{U}{2} \sum_i (\sum_a n_{ia})^2 \quad (98)$$

where c_{ia}^+ creates a hard-core boson of color a on site i , n_{ia} is the occupation number $n_{ia} = c_{ia}^+ c_{ia}$, and $c_{L+ia}^+ \equiv c_{ia}^+$.

B. Trial wave function

As already emphasized a most important aspect of any Monte Carlo scheme is the choice of a good trial wave function. To guide our choice, let us consider the exact solution at $U = 0$. In this case the ground-state is obtained by filling N independent Fermi seas consisting of planes waves with momenta $k_n = 2\pi n/L$ ($n = 0, \pm 1, \dots$). For a given type of fermion, the ground-state can be written as a Vandermonde determinant [37] and the following expression for the ground-state is obtained

$$\psi_0^{U=0}(i_1, \dots, i_P) = \prod_{l < l'} \sin\left[\frac{\pi}{L}(i_l - i_{l'})\right] \quad (99)$$

where i_1, \dots, i_P are the positions of the P fermions on the chain, $i_k = 1, \dots, L$. In terms of occupation numbers the solution can be rewritten as

$$\phi(n_1, \dots, n_L) = e^{\frac{t \vec{n} \cdot \mathcal{A}_0 \vec{n}}{2}} \quad (100)$$

where the matrix \mathcal{A}_0 of size $(L \times L)$ is given by

$$\mathcal{A}_0(i, i') = \ln \left| \sin\left[\frac{\pi}{L}(i - i')\right] \right|. \quad (101)$$

Note that (100) and (101) describe a system of particles interacting via a logarithmic potential (1D Log-gas). The exact ground-state wavefunction of the complete SU(N) model at $U = 0$ is simply obtained by writing the product of the N wavefunctions (100) associated with each color.

When the Coulomb interaction is switched on, we have chosen to take the same functional form as before for ψ_T

$$\psi_T(\vec{n}) \equiv e^{\frac{t\vec{n}A_U\vec{n}}{2}}. \quad (102)$$

Here, A_U is an arbitrary matrix of size $(NL \times NL)$. Taking into account the translational and SU(N) symmetries, at most $L + 2$ independent variational parameters can be defined. In all GFMC calculations presented in this paper the entire set of parameters has been systematically optimized. To do that, we have generalized the correlated sampling method of Umrigar *et al.* [38] along the lines presented in the preceding section. To be more precise, the set of configurations used to calculate the quantities to be minimized (variational energy or variance of \mathcal{H} , see Ref. [38]) are generated using the escape transition probability and weighted with the corresponding average trapping times. Doing this, the effective number of configurations is increased and the optimization process is facilitated. We have found that that large numbers of parameters can be easily optimized.

C. $O(L)$ algorithm

In the occupation-number representation the numerical effort for calculating the trial wave function $\psi_T(\vec{n})$ is of order $O(L^2)$. To evaluate the local energy the Hamiltonian has to be applied to the vector $|\psi_T\rangle$. Since a given configuration $|\vec{n}\rangle$ is connected by \mathcal{H} to about $O(L)$ states, the total computational cost per Monte Carlo step is about $O(L^3)$. In fact, this cost can be reduced to $O(L)$. To do that, we introduce the following set of $2NL + 1$ variables

$$(\vec{n}, \vec{n}_U, n_0) \equiv (\vec{n}, A_U\vec{n}, \frac{t\vec{n}A_U\vec{n}}{2}). \quad (103)$$

Using this representation, the wave function is given by e^{n_0} . Configurations connected by the Hamiltonian differ from each other by removing a particle of a given color a on a site i and putting it on a neighboring site j . In the occupation-number language it corresponds to add one to the component ja and remove one to the component ia of vector \vec{n} . For convenience let us introduce the vector $\vec{\delta}^{(ia)}$ whose components are zero except the component ia which is equal to one. Using the new variables just defined we have

$$\begin{aligned} & (\vec{n}, \vec{n}_U, n_0) \rightarrow \\ & (\vec{n} + \vec{\delta}^{(ja)} - \vec{\delta}^{(ia)}, \vec{n}_U + A_U\vec{\delta}^{(ja)} - A_U\vec{\delta}^{(ia)}, \\ & n_0 + \frac{t(\vec{\delta}^{(ia)} - \vec{\delta}^{(ja)})A_U(\vec{\delta}^{(ia)} - \vec{\delta}^{(ja)})}{2} - t\vec{n}_U(\vec{\delta}^{(ia)} - \vec{\delta}^{(ja)})) \end{aligned} \quad (104)$$

In the simulation the set of new variables is stored for each configuration. At each Monte Carlo step they are reactualized using (104). Finally, the numerical effort is limited to $O(L)$.

V. RESULTS

Let us now present the results for the SU(2)-, SU(3)- and SU(4) Hubbard models. SU(2) results have been obtained by solving numerically the Lieb-Wu equations [11]. Other results have been obtained with the GFMC method presented in the previous section. In all calculations we have set $t = 1$.

A. Charge gaps

The finite-size charge gap $\Delta_c(N_e, L)$ is defined as

$$\Delta_c(N_e, L) \equiv$$

$$E_0(N_e + 1, L) + E_0(N_e - 1, L) - 2E_0(N_e, L) \quad (105)$$

where $E_0(N_e, L)$ is the total ground-state energy of a ring of length L with N_e electrons. In this expression $N_e \pm 1$ means that a fermion of an arbitrary color is added to or removed from the system. Denoting N the number of colors, calculations are done for a number of fermions of each color equal to L/N , and therefore for a total density $n \equiv N_e/L$ equal to one. In order to get the exact charge gap the limit $L \rightarrow \infty$ must be performed. As usual this is done by calculating charge gaps for different sizes and extrapolating to infinity. Here, SU(3) and SU(4) calculations have been done for $L = 9, 12, 18, 27$ and $L = 8, 16, 24, 32$, respectively. The finite-size gaps have been found to converge almost linearly as a function of the inverse of the size. Accordingly, the limit $L \rightarrow \infty$ of the gap has been obtained from a fit of the data with a linear or quadratic function of $1/L$. Figure 1 presents the charge gaps obtained for $N = 2, 3, 4$ as a function of the Coulomb interaction U .

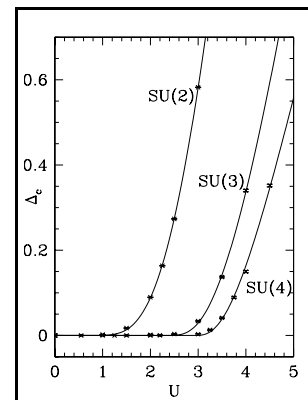


Fig. 1. Charge gaps as a function of the interaction U for the SU(2), SU(3), and SU(4) Hubbard models. The values of the gaps have been extrapolated to $L \rightarrow \infty$ (see text).

A first important remark concerns the quality of the Monte Carlo simulations. As it can be seen in Fig. 1, the error bars on the different gaps are quite small. A typical value is about 0.001. Errors are small because total energies are calculated with a very high level of accuracy. For example, for the SU(4)-model with $L = 32$ and $U = 0.5$, we get $E_0(32, 32) = -52.13056(15)$ for a total number of elementary Monte Carlo steps equal to $8 \cdot 10^7$. Clearly, the relative error of about $3 \cdot 10^{-6}$ is very small. In the large U -regime where the trial wave function is not expected to be as good as for small U , we still get excellent results. For example, for $U = 4.5$ we get $E_0(32, 32) = -23.7118(13)$ (1.610^8 MC steps) with a relative error of about $6 \cdot 10^{-5}$. Using the standard GFMC method (presented in Sec. III.A) we get, for $U = 0.5$, $E_0(32, 32) = -52.13050(40)$ and, for $U = 4.5$, $E_0(32, 32) = -23.7210(110)$ (in both cases the maximum time-step allowed has been chosen, see Eq. (70)). The improvement resulting from the new approach, particularly at large U , is noticeable. Finally, using the approach of Trivedi and Ceperley [19] (introduction of the Poisson process but no integration in time) we get for $U = 0.5$ $E_0(32, 32) = -52.13041(22)$ and for $U = 4.5$, $E_0(32, 32) = -23.7121(30)$. These results illustrate the improvement resulting from the time integration.

Having at our disposal such accurate results we can try to find out whether or not a gap opens for a non-zero value of U . Considering only continuous transitions, two scenarios are possible. A first possibility is to open a gap for any non-zero value of U . In that case we write the gap versus U as follows

$$\Delta_c = C \exp(-G/U). \quad (106)$$

A second scenario consists in looking for the existence of a KT-type transition at a finite value U_c of the Coulomb interaction. In that case the gap is written as

$$\Delta_c = C_{KT} \exp\left(-\frac{G_{KT}}{\sqrt{U - U_c}}\right) \quad (107)$$

for $U > U_c$ and zero otherwise. The three sets of results have been fitted either using Eqs. (106) or (107). The fitting procedure used is a standard one, based on the minimization of a chi-square type function including statistical errors. Our most important conclusion is that all sets of data can be correctly represented within our small statistical errors either using the gapful representation, Eq. (106), or using a KT scenario, Eq. (107) with a not too large value of U_c . For example, using Eq. (106) possible representations are $(C = 25.313, G = 11.318)$, $(C = 274.634, G = 26.745)$, and $(C = 515.649, G = 32.755)$, for $N = 2, 3$, and 4 , respectively. Although no clear physical content can be given to the magnitude of coefficients, it is nevertheless satisfactory to verify that in the case of SU(2), the gapful (106) leads to not too large values for the coefficients. This should be contrasted with the SU(3) and SU(4) cases for which the parameters are important. Within a KT scenario all data can also be

very well fitted. In the case of SU(2) where we know for sure that no KT transition exists, the ‘critical value’ issued from our fits ranges from 0 to about 0.5. For example, a possible representation is given by $(C_{KT} = 541.310, G_{KT} = 11.053, \text{ and } U_c = 0.384)$. For the SU(3)-model accurate representations can be obtained with a value of U_c ranging from 0 to about 2.3 For $U_c = 2.2$ (the value we shall propose later for the critical value) we get: $(C_{KT} = 45.050, G_{KT} = 6.567, \text{ and } U_c = 2.2)$. For SU(4) the interval is larger. Allowed values range from 0 to about 2.9. For $U_c = 2.8$ (our proposed value, see below) we get: $(C_{KT} = 17.889, G_{KT} = 5.144, \text{ and } U_c = 2.8)$. In contrast with the gapful representation, it should be noted that coefficients are now much larger for the SU(2) model than for the SU(3) and SU(4) models.

In conclusion, using accurate values of the gaps no conclusions can be reasonably drawn about the existence or not of a KT-type transition at a finite value of U . Numerical evidences based on other quantities are therefore called for (see next sections). From the fitting of our data the only conclusion we are allowed to draw is that a KT-transition is only possible within the range (0,2.3) for SU(3) and within the range (0,2.9) for SU(4). In addition to this, if such a transition actually occurs in both models, we should expect a difference for the critical values given by: $U_c[SU(4)] - U_c[SU(3)] \sim 0.5 - 0.6$ (see Fig. 1).

B. Spin gap

The spin gap is defined as the change in ground-state energy produced when destroying a fermion of a given color and creating a fermion of a different color (in the SU(2) case it consists in flipping one spin). Note that in this process the charge number is kept fixed. For a finite system we have

$$\Delta_s(N_e, L) \equiv E_0(N_e + 1, L) - E_0(N_e - 1, L) \quad (108)$$

where $N_e \pm 1$ involves an arbitrary pair of electrons of different colors.

For the SU(2) case the system is known from the exact solution to be gapless for an arbitrary value of the interaction strength U . For a number of colors greater than 2, it is an open question. This is an important point since the existence of a gapful regime would very likely indicate the existence of a coupling between spin and charge degrees of freedom. In all calculations performed for $N=3$ and 4 , and for a coupling constant U ranging from very small to very large values (up to $U = 10$) no evidence for the existence of such a gap has been found. Thus, it can be quite safely concluded that the spin sector of SU(N) $N = 2, 3, 4$ is gapless for an arbitrary interaction in full agreement with the bosonization prediction. To illustrate this point we present in Fig. 2 a typical behavior for the spin gap of SU(3) as a function of $1/L$ at the relatively large value $U = 4.5$ (at least two times greater

than the maximal value expected for U_c in the charge sector). The behavior of the gap is essentially linear and extrapolation to the origin leads to a vanishing gap.

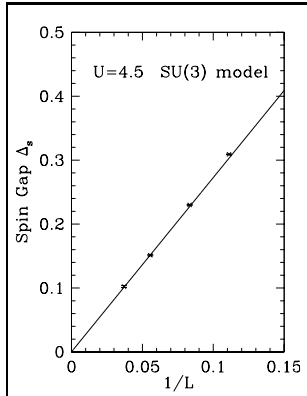


Fig. 2. Spin gap as a function of $1/L$ for the SU(3) Hubbard model at $U = 4.5$. The solid line is a linear fit of the data.

C. Luttinger liquid parameters

In this section we present calculations of the Luttinger liquid parameters u_c and K_c . For that we shall make use of their relations with the compressibility κ and charge stiffness D_c of the system. For a model with N colors (SU(N)) we have the following relations

$$\frac{\pi u_c}{K_c} \kappa n^2 = \frac{N}{2} \quad (109)$$

and

$$D_c = N u_c K_c \quad (110)$$

where $n = N_e/L$ (N_e total number of electrons) is the electron density. The compressibility κ is defined as the second derivative of the ground-state energy E_0 with respect to the density of particles

$$\frac{1}{\kappa} = \frac{1}{L} \frac{\partial^2 E_0}{\partial n^2}. \quad (111)$$

A convenient finite-size approximation of the compressibility is

$$\kappa = \frac{L}{N_e^2} \left(\frac{E_0(N_e + N, L) + E_0(N_e - N, L) - 2E_0(N_e, L)}{N^2} \right)^{-1} \quad (112)$$

where $N_e \pm N$ in E_0 means that N fermions -one of each color- are added to or removed from the system.

The charge stiffness is given by

$$D_c = \frac{\pi}{L} \left. \frac{\partial^2 E_0}{\partial \varphi^2} \right|_{\varphi=0} \quad (113)$$

where φ is a charge twist in the system. This charge twist is imposed by introducing the following twisted boundary conditions

$$c_{i+La}^+ = e^{i\varphi} c_{ia}^+, \quad (114)$$

for an arbitrary site i and color a .

By calculating with GFMC total ground-state energies for different numbers of electrons, formula (112) allows a direct calculation of the compressibility. In contrast, the GFMC calculation of the charge stiffness is more tricky due to the presence of a complex hopping term at the boundary. To circumvent this difficulty we resort to the second-order perturbation-theory expression of the charge stiffness. We have

$$D_c = \frac{\pi}{L} \left(\langle -T \rangle - 2 \sum_{k \neq 0} \frac{|\langle k | J | 0 \rangle|^2}{E_k - E_0} \right) \quad (115)$$

where $T = -t \sum (c_{i+1a}^+ c_{ia} + H.c.)$ is the kinetic-energy operator, $J = -it \sum (c_{i+1a}^+ c_{ia} - H.c.)$ is the paramagnetic current operator, $\langle \dots \rangle$ denoting the expectation value in the ground-state, all quantities being evaluated at $\varphi = 0$. To evaluate the kinetic term we make use of the Hellman-Feynman theorem: $\langle T \rangle = E_0 - U \frac{\partial E_0}{\partial U}$. In practice, the following finite-difference expression is used

$$\langle T \rangle = E_0 - U \left(\frac{E_0(U + \delta U) - E_0(U - \delta U)}{2\delta U} \right) \quad (116)$$

with δU small enough to make higher-order contributions negligible.

The second-order part of formula (115) can be re-interpreted back as the second-derivative of the total ground-state energy of a new Hamiltonian consisting of the original Hamiltonian plus a perturbation associated with the flux operator J . This leads to the following relation

$$\sum_{k \neq 0} \frac{|\langle k | J | 0 \rangle|^2}{E_0 - E_k} = \frac{1}{2} \frac{\partial^2 \tilde{E}_0(\lambda)}{\partial \lambda^2} \quad (117)$$

where \tilde{E}_0 is the ground-state energy of the new Hamiltonian defined by

$$\tilde{H} = -(t + \lambda) \sum_{ia} (c_{i+1a}^+ c_{ia}) - (t - \lambda) \sum_{ia} (c_{i-1a}^+ c_{ia}) + V(U) \quad (118)$$

and $V(U)$ is the potential part of the problem. Using formulas (117) and (118) the charge stiffness can now be obtained from a series of GFMC ground-state calculations of total energies of real Hamiltonians (more precisely, E_0 , $E_0(\delta U)$, and $E_0(-\delta U)$ for \mathcal{H} , and $\tilde{E}_0(\lambda)$ for

\tilde{H} , Eq. (118)). It should be emphasized that the new Hamiltonian \tilde{H} is real but not symmetric: Left-moving and right-moving electrons do not have the same velocity. Of course, such a property is easily implemented within a QMC framework.

Figures [3,4,5,6,7,8] present the Luttinger parameters u_c and K_c for the SU(2), SU(3), and SU(4) Hubbard models as a function of the interaction U and for different sizes L . For the SU(2) model, parameters have been obtained by computing ground-state energies issued from the standard Lieb-Wu equations (computation of the compressibility, formula (112)) and from their generalization to the case of twisted boundary conditions as presented by Shastry and Sutherland [39] (computation of the charge stiffness, formula (113)). For the SU(3) and SU(4) models we have followed the general route just presented above.

A first striking result emerging from the figures is the strong qualitative differences between the general behavior of Luttinger parameters of the SU(2) model on the one hand, and of the SU(3) and SU(4) models, on the other hand. Let us first have a look at the charge velocity u_c .

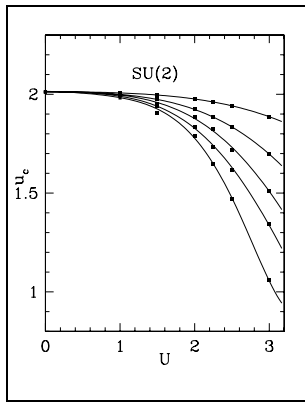


Fig. 3. u_c as a function of U for the SU(2) Hubbard model.

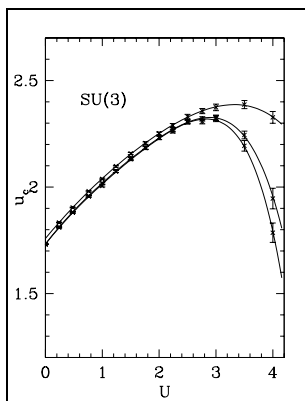


Fig. 4. u_c as a function of U for the SU(3) Hubbard model.

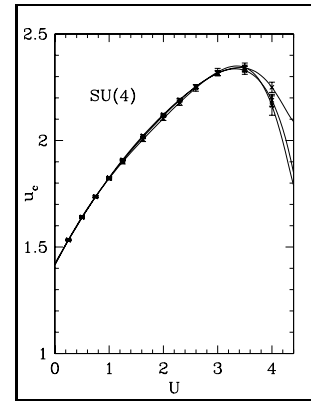


Fig. 5. u_c as a function of U for the SU(4) Hubbard model.

In the SU(2) case the charge velocity has been calculated for various values of U and for the sizes $L = 6, 10, 14, 18,$ and 22 . Results are presented in Fig. 3. The upper curve corresponds to $L = 6$, the lower one to the maximum size, $L = 22$. In between, the curves are ordered according to the magnitude of L . For a given size L , the charge velocity is found to decrease as a function of U . For a given U , u_c also decreases as a function of the size L . Such a behavior is quite typical of a gapped system in which collective charge excitations are damped away. In the limit of large sizes, the charge velocity is expected to vanish for a non-zero value of the interaction.

The charge velocities of the SU(3) model, Fig. 4, and of the SU(4) model, Fig. 5, display a very similar behavior which is dramatically different from the one observed for SU(2). Starting from their free value at $U = 0$ ($u_c = \sqrt{3}$ and $u_c = \sqrt{2}$ for SU(3) and SU(4), respectively), they increase as a function of U with a finite slope at the origin. After some critical value of U both velocities go down quite rapidly. In the first part of the curves (small and intermediate values of U) the charge velocity is found to converge quite rapidly as a function of the size. All curves presented cannot be distinguished within statistical errors. Although the calculations presented here are limited to systems with a maximum size of $L = 27$ (SU(3)) or $L = 32$ (SU(4)) some preliminary calculations at larger sizes strongly suggest that the values plotted are indeed converged. Such results strongly support the existence of a gapless phase for the SU(3) and SU(4) models. At larger values of U the situation is rather different. The charge velocities decrease quite rapidly both as a function of U and as a function of L . This behavior indicates the existence of a gapped phase. In order to be more quantitative let us have a look at the value of the slope at the origin. The theoretical prediction can be obtained from Eqs. (38). For SU(3) calculations have been done for the sizes $L=9, 18,$ and 32 . The slope at the origin is found to be $0.32(1), 0.32(1),$ and $0.33(2)$ for $L=9, 18,$ and 27 , respectively. These results are in perfect agreement with the theoretical prediction

of $\frac{1}{\pi} \simeq 0.318$. For the SU(4) model calculations have been done for the sizes $L=16,24$, and 32 . The slope at the origin is found to be $0.46(1), 0.47(1)$, and $0.45(2)$ for $L=16,24$, and 32 , respectively. Here also, the results are in perfect agreement with the theoretical prediction of $\frac{3}{2\pi} \simeq 0.477$. Let us now consider our results for K_c .

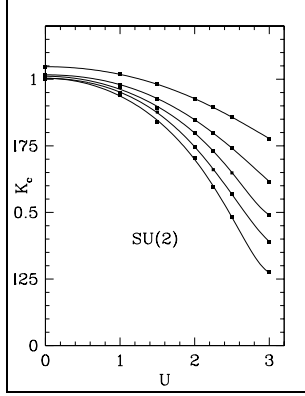


Fig. 6. K_c as a function of U for the SU(2) Hubbard model.

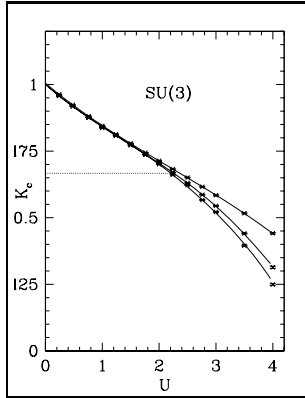


Fig. 7. K_c as a function of U for the SU(3) Hubbard model.

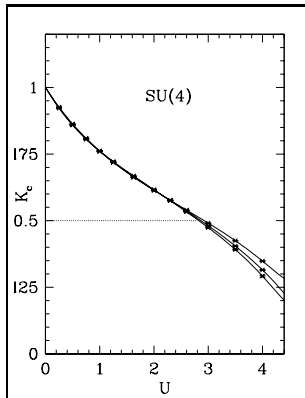


Fig. 8. K_c as a function of U for the SU(4) Hubbard model.

Here also, there exists a common behavior for the cases SU(3) and SU(4), and a different one for SU(2). In the latter case, Fig. 6, K_c decreases either as a function of U or as a function of the size. The slope at the origin, $U = 0$, is essentially zero and K_c is expected to vanish at large sizes, except, of course, in the free case. Once again, this behavior is typical of a gapped system. In the two other cases, the situation is rather different. In the same way as for the charge velocity, two regimes can be distinguished, see Figs. 7 and 8. At small and intermediate U , the values of K_c are found to be very well converged within statistical errors as a function of the size L . The curve is smooth with a finite slope at the origin. In the second regime corresponding to larger values of U the curves K_c versus U go down as a function of the size. Clearly, this latter regime corresponds to a gapped phase. Having nearly exact values of K_c up to some critical value U_c for SU(3) and SU(4), the next logical step consists in comparing these values to the predictions of bosonization. A first important prediction was the opening of a gap in the charge sector for a value of K_c equal to $2/N$, Eq. (51). In Fig. 7 corresponding to the SU(3) case, a dashed line has been drawn at the value $K_c = 2/3$. The intersection of this line with the curves of K_c appears at about $U_c \sim 2.2$. A most remarkable result is that this value of U is both consistent with the critical value extracted from the calculation of the charge gaps, Fig. 1, but also with the fact that it lies in the domain of U where the values of K_c begin not to converge as a function of the size (a fact usually interpreted as resulting from the existence of a finite correlation length). A very similar situation is obtained in the SU(4) case. Using the same type of arguments, U_c is found to be around 2.8. When studying charge gaps we had observed a difference of U_c , Fig. 1, between SU(3) and SU(4) of between 0.5 and 0.6. This is in very good agreement with what is found here from independent data on K_c . A second prediction which can be tested is the estimate of the value of U_c itself. Formula (52) gives

$$U_c = \frac{\pi}{2} \frac{N^2 - 4}{N - 1} \sin \frac{\pi}{N}.$$

For $N = 3$ and $N = 4$ one gets $U_c = 3.40$ and $U_c = 4.44$, respectively. As already pointed out, these estimates must be considered with caution. However, it should give the correct trend as a function of N . Here, if we look at the ratio $U_c[SU(4)]/U_c[SU(3)]$ we get about 1.31 from the theoretical estimate and about 1.27 from our data. The agreement is excellent. Another point which can be checked is the value of the slope at the origin. For the SU(3) case, it is found to be $-0.18(1), -0.19(1)$, and $-0.19(2)$ for $L=9,18$, and 27 , respectively. These results are in very good agreement with the theoretical prediction of $-\frac{1}{\sqrt{3}\pi} \simeq -0.183$ given by Eq. (38). For SU(4) we find a slope of $-0.31(1), -0.33(1)$, and $-0.32(2)$ for $L=16,24$, and 32 , respectively. These results are also in total agreement with the theoretical prediction

of $-\frac{3}{2\sqrt{2}\pi} \simeq -0.337$.

Finally, it can be very useful for interested readers to give some compact and accurate representations of the Luttinger parameters K_c and u_c as a function of U . For both parameters a minimal representation we may think of (see section II.B) is

$$K_c = \frac{1}{\sqrt{1 + k_1 U + k_2 U^2}}$$

$$u_c = v_F \sqrt{1 + u_1 U + u_2 U^2}. \quad (119)$$

For SU(3) we obtain

$$k_1 = 0.33452, k_2 = 0.08789$$

$$u_1 = 0.37929, u_2 = -0.025509.$$

Note that these values are not too far from the bare values corresponding to Eqs. (37), $k_1^0 = u_1^0 = \frac{2}{\pi v_F} \simeq 0.36755$, $k_2^0 = u_2^0 = 0$.

For SU(4) we obtain

$$k_1 = 0.62065, k_2 = 0.12298$$

$$u_1 = 0.71486, u_2 = -0.052705$$

to compare to the bare values given by $k_1^0 = u_1^0 = \frac{3}{\pi v_F} = 0.675237$, $k_2^0 = u_2^0 = 0$.

As already discussed we have found no evidences for the opening of a spin gap in the case of the SU(3) and SU(4) models. In other words, the system remains critical with respect to the spin degrees of freedom for any value of the interaction. For these models the slope at the origin is predicted to be equal to $-\frac{1}{2\pi} \simeq -0.159$ (Eq. (27)). Once again, this value has been recovered using our numerical data. To compute the spin velocity we have used the formula expressing the spin gap as a function of the size for a critical system [28]

$$u_s = \frac{\Delta_s(N_e, L)}{2\pi L}. \quad (120)$$

For SU(3) and SU(4) we get for the slope -0.18(2) and -0.18(3), respectively, in very good agreement with the theoretical prediction.

A final piece of information which can be extracted from our data is related to the way the total ground-state energy converges to its asymptotic value. To be more precise, it is known that the ground-state energy per site, $e_0(L)$, of a Luttinger liquid is expected to behave as follows [28]

$$e_0(L) \simeq e_0(+\infty) - \frac{\pi}{6L^2} \sum_i u_i \quad (121)$$

where $\sum_i u_i$ denotes the total velocity associated with all critical excitations. In the free case, N degrees of freedom

are critical, and the total velocity is equal to Nv_F . When the interaction is turned on, it is possible to follow the evolution of the total velocity as a function of U . This has been done for the SU(3) model. Taking our data for the sizes $L=9, 18$, and 27 the ground-state energy has been fitted with a form adapted to Eq. (121), $e_0 = a - b/L^2$. From this fit an effective number of critical modes can be defined as follows

$$N_{eff} = \frac{6b}{\pi v_F}.$$

The result is presented in Fig (9).

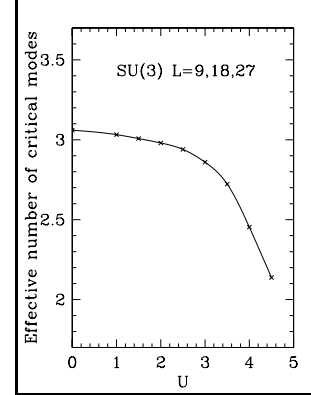


Fig. 9. Effective number of critical modes as a function of U for the SU(3) Hubbard model.

Although the transition is not as sharp as for the Luttinger parameters, the loss of one critical mode (passing from 3 to 2) is clearly seen when U varies from zero to infinity. A similar curve may be obtained for the SU(4) case.

VI. CONCLUDING REMARKS

In this work, we have studied the SU(N) generalization of the one-dimensional Hubbard model for repulsive interaction at half-filling. Using a combination of bosonization and QMC results, we have clearly shown that the SU(N) Hubbard model for $N > 2$ behaves very differently from the SU(2) case. Strong numerical and theoretical evidences have been given in favor of a Mott transition, between a metallic and an insulating phase, occurring for a finite value of the Coulomb repulsion $U_c > 0$ for $N > 2$.

The picture emerging from the bosonization approach consists in a spin-charge separation at low energy. The spin degrees of freedom are critical for arbitrary U and described by the SU(N)₁ WZNW model with a central charge $c = N - 1$ ($N - 1$ gapless bosonic modes). The effective theory associated with the charge degrees of freedom corresponds to a sine-Gordon model at $\beta^2 = 4\pi N K_c(U)$. For a small value of the Coulomb interaction U , the interaction is irrelevant. The charge sector

is then critical and described by a massless bosonic field. In this weak coupling phase, the system is metallic with anomalous power law behaviors in the physical quantities typical of a Luttinger liquid. For a finite value of the interaction U_c such that $K_c(U_c) = 2/N$, a KT phase transition to an insulating phase is expected in the bosonization approach. In this strong-coupling phase, the charge bosonic field becomes locked and the infinite discrete Z_∞ symmetry related to the periodicity of the potential of the sine-Gordon model is spontaneously broken. The only degrees of freedom that remain critical in this strong coupling phase are the $N - 1$ spin modes and after integrating out the massive charge degrees of freedom, the low-energy theory of the model corresponds to the SU(N) Heisenberg antiferromagnet.

Very accurate numerical simulations based on a generalization of the GFMC method and fully optimized trial wave functions have been performed to obtain the spin and charge gaps, and the Luttinger liquid parameters as a function of the Coulomb interaction for the SU(2), SU(3), and SU(4) Hubbard models. A metal-insulator phase transition at a finite value U_c is clearly seen for SU(3) ($U_c \sim 2.2$) and SU(4) ($U_c \sim 2.8$) in contrast with the standard SU(2) case. In addition all the results obtained for $N = 3$ and $N = 4$ are fully consistent with the theoretical framework drawn in section II. This provides an accurate test of the bosonization approach to the SU(N) Hubbard model for small and large values of U . It is therefore natural to expect that the physical picture emerging from the two cases studied here can be extended to *arbitrary* values of N . Thus one may conclude that the occurrence at a finite value of the interaction of a Mott transition of the KT type is *generic* in the SU(N) Hubbard model for $N > 2$ at half-filling. In addition, it should be emphasized that the calculations of the Luttinger parameters K_c and u_c presented in Sec. II.B are of very good quality (in particular they are converged as a function of the size) and thus provide an accurate characterization of the low-energy properties of the metallic phase of the SU(3) and SU(4) Hubbard models.

Let us now compare our results with the exact solution of the integrable model based on the SU(N) generalization of the Lieb-Wu Bethe ansatz equations [12]. As discussed in the introduction, an exact solution of an SU(N) generalization of the Hubbard model is available. Although the underlying lattice Hamiltonian of the model is not known, it involves very likely long-range interactions that dynamically exclude three-electron configurations. The question that naturally arises is whether the physics described by the latter model is similar, when $N > 2$, to that of the lattice SU(N) Hubbard model that we have studied in this paper. At half-filling, the SU(N) integrable model undergoes a *first-order* phase-transition, as one varies U , from a metallic to an insulating phase [13]. This is in disagreement with the KT transition predicted by our analysis. In the metallic phase the integrable model is a Luttinger liquid for every N [13,41] with the same physical properties as those obtained by

the bosonization approach for the SU(N) Hubbard model. However, the charge stiffness K_c obtained from the Bethe ansatz equations varies between $1/N$ and 1 as U decreases from U_c to 0 [13,41]. The value at the transition ($K_c = 1/N$) is thus two times larger than the value obtained for the SU(N) Hubbard model. This clearly confirms that the integrable model differs from the lattice SU(N) Hubbard model in the charge sector. As already pointed out, this difference should result from the presence of non-local interactions in the lattice model associated with the integrable SU(N) model.

Regarding perspectives, it is clearly of interest to further explore the phase diagram of the SU(N) Hubbard model: case of an attractive interaction, dependence on the filling, etc... For an attractive interaction at half-filling, bosonization predicts that a phase transition should also occur as $|U|$ varies. For incommensurate fillings, it is easy to see, within the bosonization framework, that the system is a Luttinger liquid for arbitrary N and positive U where the leading asymptotics of the electronic Green's function and spin-spin correlation coincide with those computed in the metallic phase. The situation is less clear for commensurate fillings $k_F = \pi n/(Na_0)$ (N/n being an integer). In the bosonization approach, a gap opens in the charge sector for $K_c = 2n^2/N$. The existence of a Mott transition for commensurate fillings clearly requires the full knowledge of $K_c(U, n)$ of the lattice model. Some preliminary calculations show that there is a very special commensurate filling, $n = N/2$, where no Mott transition exists and for which the charge and spin degrees of freedom are massive for $N > 2$ and arbitrary U [40].

Let us end by noting a very interesting connection between the metal-insulator transition predicted in the SU(N) Hubbard model and the existence of plateaux in magnetization curves of spin ladders under a strong magnetic field [42–44]. Using the Jordan-Wigner transformation, one can indeed interpret the SU(N) Hubbard model as a N-leg S=1/2 XY spin ladder in a uniform magnetic field along the z-axis and coupled in a symmetric way by Ising interaction. The relation between the Fermi momenta and the magnetization $\langle M \rangle$ (normalized such that the saturation value is ± 1) is: $k_F = \pi(1 - \langle M \rangle)/(2a_0)$. The Mott transition found in this work for the SU(N) Hubbard model at half-filling corresponds to the appearance of plateaux at $\langle M \rangle = (N - 2)/N$ in the magnetization curves of the previous N-leg XY spin ladder. Moreover, the existence of a Mott transition for the SU(N) Hubbard model at commensurate filling will give additional plateaux located at $\langle M \rangle = (N - 2n)/N$ in the magnetization curves of the corresponding spin ladder.

Acknowledgments: We would like to thank A. O. Gogolin and A. A. Nersisyan for valuable discussions and for a related collaboration. This work was supported by the “Centre National de la Recherche Scientifique” (C.N.R.S.)

APPENDIX:

In this Appendix, we give some details of computations to establish the separation of spin and charge (24) at the Hamiltonian level in the continuum limit of the SU(N) Hubbard model and fix the expressions of $u_{c,s}$ and $G_{c,s}$ given by Eqs. (27, 28).

1. Sugawara form of the free Hamiltonian

To begin with, we shall recall some basic things on the SU(N) non-Abelian bosonization (for a review see Refs. [23,24,26]). As seen in section IIA, the chiral SU(N) spin current $\mathcal{J}_{R,L}^A$ can be expressed in terms of N left-right moving fermions $\psi_{aR,L}$:

$$\mathcal{J}_{R(L)}^A =: \psi_{aR(L)}^\dagger \mathcal{T}_{ab}^A \psi_{bR(L)} :. \quad (\text{A1})$$

The left (respectively right)-moving fermions are holomorphic (respectively anti-holomorphic) fields of the complex coordinate ($z = \tau + ix$, τ being the imaginary time): $\psi_{aL}(z), \psi_{aR}(\bar{z})$. These fields are defined by the following OPEs:

$$\begin{aligned} \psi_{aL}^\dagger(z) \psi_{bL}(\omega) &\sim \frac{\delta_{ab}}{2\pi(z-\omega)} \\ +: \psi_{aL}^\dagger \psi_{bL} :(\omega) + (z-\omega) : \partial \psi_{aL}^\dagger \psi_{bL} :(\omega) + .. \\ \psi_{aR}^\dagger(\bar{z}) \psi_{bR}(\bar{\omega}) &\sim \frac{\delta_{ab}}{2\pi(\bar{z}-\bar{\omega})} \\ +: \psi_{aR}^\dagger \psi_{bR} :(\bar{\omega}) + (\bar{z}-\bar{\omega}) : \bar{\partial} \psi_{aR}^\dagger \psi_{bR} :(\bar{\omega}) + .. \end{aligned} \quad (\text{A2})$$

with $\partial = \partial_\omega, \bar{\partial} = \partial_{\bar{\omega}}$ and there are no singularities in the OPE when one does the fusion of two operators belonging to different sectors.

Let us now consider the OPE between two left SU(N) spin currents for instance:

$$\begin{aligned} \mathcal{J}_L^A(z) \mathcal{J}_L^B(\omega) &=: \psi_{aL}^\dagger \mathcal{T}_{ab}^A \psi_{bL} : (z) : \psi_{dL}^\dagger \mathcal{T}_{de}^B \psi_{eL} : (\omega) \\ &= \mathcal{T}_{ab}^A \mathcal{T}_{de}^B \psi_{aL}^\dagger(z) \psi_{eL}(\omega) \psi_{bL}(z) \psi_{dL}^\dagger(\omega). \end{aligned} \quad (\text{A3})$$

Using the OPEs (A2), the commutation relation (6), and the normalization of the generators of the SU(N) Lie algebra, one obtains:

$$\begin{aligned} \mathcal{J}_L^A(z) \mathcal{J}_L^B(\omega) &\sim \frac{\delta^{AB}}{8\pi^2(z-\omega)^2} \\ &+ \frac{if^{ABC}}{2\pi(z-\omega)} \mathcal{J}_L^C(\omega). \end{aligned} \quad (\text{A4})$$

In the same way, we find for the right spin current:

$$\begin{aligned} \mathcal{J}_R^A(\bar{z}) \mathcal{J}_R^B(\bar{\omega}) &\sim \frac{\delta^{AB}}{8\pi^2(\bar{z}-\bar{\omega})^2} \\ &+ \frac{if^{ABC}}{2\pi(\bar{z}-\bar{\omega})} \mathcal{J}_R^C(\bar{\omega}). \end{aligned} \quad (\text{A5})$$

Evaluating these OPE at equal time, one recovers the OPE (15) showing that $\mathcal{J}_{R,L}^A$ are SU(N)₁ spin current. With the same procedure, one can compute the OPE between the charge current $\mathcal{J}_{R,L}^0$ using its definition (17) in terms of the underlying fermions:

$$\begin{aligned} \mathcal{J}_L^0(z) \mathcal{J}_L^0(\omega) &\sim \frac{N}{4\pi^2(z-\omega)^2} \\ \mathcal{J}_R^0(\bar{z}) \mathcal{J}_R^0(\bar{\omega}) &\sim \frac{N}{4\pi^2(\bar{z}-\bar{\omega})^2} \end{aligned} \quad (\text{A6})$$

so that the charge current $\mathcal{J}_{R,L}^0$ belongs to the U(1)_N KM algebra.

The next step is to obtain the Sugawara form (20, 21) of the free part of the Hamiltonian (\mathcal{H}_0). Let us consider, for instance, the left sector of the theory since we shall obtain the same result for the right part with the substitution: $L \rightarrow R, (z, \omega) \rightarrow (\bar{z}, \bar{\omega})$ and $\partial \rightarrow \bar{\partial}$. We need now the following OPE for the spin sector:

$$\begin{aligned} \mathcal{J}_L^A(z) \mathcal{J}_L^A(\omega) &=: \psi_{aL}^\dagger \mathcal{T}_{ab}^A \psi_{bL} : (z) : \psi_{dL}^\dagger \mathcal{T}_{de}^A \psi_{eL} : (\omega) \\ &= \frac{1}{2} \left(\delta_{ae} \delta_{bd} - \frac{1}{N} \delta_{ab} \delta_{de} \right) \psi_{aL}^\dagger(z) \psi_{eL}(\omega) \psi_{bL}(z) \psi_{dL}^\dagger(\omega) \end{aligned} \quad (\text{A7})$$

where we have used the relation (8). Using (A2) and keeping also the first regular terms in the fusion, we get:

$$\begin{aligned} \mathcal{J}_L^A(z) \mathcal{J}_L^A(\omega) &\sim \frac{1}{8\pi^2(z-\omega)^2} \\ &+ \frac{N+1}{2N} : \psi_{aL}^\dagger \psi_{aL} \psi_{bL} \psi_{bL}^\dagger : (\omega) \\ &- \frac{N^2-1}{2\pi N} : \psi_{aL}^\dagger \partial \psi_{aL} : (\omega). \end{aligned} \quad (\text{A8})$$

Therefore, one obtains:

$$\begin{aligned} : \mathcal{J}_L^A \mathcal{J}_L^A : &:= \frac{N+1}{2N} : \psi_{aL}^\dagger \psi_{aL} \psi_{bL} \psi_{bL}^\dagger : \\ &- \frac{N^2-1}{2\pi N} : \psi_{aL}^\dagger \partial \psi_{aL} :. \end{aligned} \quad (\text{A9})$$

In the same way, we obtain for the left charge current:

$$: \mathcal{J}_L^0 \mathcal{J}_L^0 : := - : \psi_{aL}^\dagger \psi_{aL} \psi_{bL} \psi_{bL}^\dagger : - \frac{1}{\pi} : \psi_{aL}^\dagger \partial \psi_{aL} :. \quad (\text{A10})$$

One can eliminate the four fermions terms by considering the following combination:

$$\frac{\pi}{N} : \mathcal{J}_L^0 \mathcal{J}_L^0 : + \frac{2\pi}{N+1} : \mathcal{J}_L^A \mathcal{J}_L^A : := - : \psi_{aL}^\dagger \partial \psi_{aL} :. \quad (\text{A11})$$

Since one has $\partial \psi_{aL} = -i\partial_x \psi_{aL}$ within our convention, the identity (A11), the so-called Sugawara form, states that the free Hamiltonian of N relativistic left-moving fermions can be written only as a function of left current-current terms. In the right part, we have also a similar identity:

$$\frac{\pi}{N} : \mathcal{J}_R^0 \mathcal{J}_R^0 : + \frac{2\pi}{N+1} : \mathcal{J}_R^A \mathcal{J}_R^A : = -i : \psi_{aR}^\dagger \partial_x \psi_{aR} : \dots \quad (\text{A12})$$

Collecting all terms, we finally obtain the Sugawara form of the free Hamiltonian \mathcal{H}_0 (10):

$$-i \left(: \psi_{aR}^\dagger \partial_x \psi_{aR} : - : \psi_{aL}^\dagger \partial_x \psi_{aL} : \right) = \frac{\pi}{N} \left(: \mathcal{J}_R^0 \mathcal{J}_R^0 : + \mathcal{J}_L^0 \mathcal{J}_L^0 : \right) + \frac{2\pi}{N+1} \left(: \mathcal{J}_R^A \mathcal{J}_R^A + \mathcal{J}_L^A \mathcal{J}_L^A : \right). \quad (\text{A13})$$

2. Sugawara form of the SU(N) Hubbard Hamiltonian

We shall now investigate the effect of the Hubbard interaction in the continuum limit to fix the expressions (27) and (28) of the velocities ($u_{c,s}$) and the coupling constants ($G_{c,s}$). Using the continuum description of the SU(N) spin density (12), the interacting part (7) is given by dropping all oscillatory contributions:

$$\mathcal{V}_0 = -\frac{U a_0 N}{N+1} \left(: \mathcal{J}^A : : \mathcal{J}^A : + : \mathcal{N}^A : : \mathcal{N}^{A\dagger} : + : \mathcal{N}^{A\dagger} : : \mathcal{N}^A : \right). \quad (\text{A14})$$

The OPE between the $2k_F$ parts of the spin density can be computed using (13) and (A2) as in the previous subsection. We find up to constant terms:

$$\begin{aligned} & : \mathcal{N}^A : (z, \bar{z}) : \mathcal{N}^{A\dagger} : (\omega, \bar{\omega}) + : \mathcal{N}^{A\dagger} : (z, \bar{z}) : \mathcal{N}^A : (\omega, \bar{\omega}) \\ & \sim -\frac{N^2-1}{2\pi N} \frac{z-\omega}{\bar{z}-\bar{\omega}} : \psi_{aL}^\dagger \partial \psi_{aL} : (\omega) \\ & - \frac{N^2-1}{2\pi N} \frac{\bar{z}-\bar{\omega}}{z-\omega} : \psi_{aR}^\dagger \bar{\partial} \psi_{aR} : (\bar{\omega}) \\ & - : \psi_{aL}^\dagger \psi_{aL} \psi_{bR}^\dagger \psi_{bR} : (\omega, \bar{\omega}) \\ & + \frac{1}{N} : \psi_{aL}^\dagger \psi_{bL} \psi_{bR}^\dagger \psi_{aR} : (\omega, \bar{\omega}). \end{aligned} \quad (\text{A15})$$

Using Eqs. (A9, A10) and similar equations in the right sector together with the definition of the charge current (17), we end with:

$$\begin{aligned} \mathcal{J}^A \mathcal{J}^A + \mathcal{N}^A \mathcal{N}^{A\dagger} + \mathcal{N}^{A\dagger} \mathcal{N}^A & \sim -\frac{N^2-1}{2N^2} \left(: \mathcal{J}_R^0 \mathcal{J}_R^0 + \mathcal{J}_L^0 \mathcal{J}_L^0 : \right) \\ & + \frac{1}{N} \left(: \mathcal{J}_R^A \mathcal{J}_R^A + \mathcal{J}_L^A \mathcal{J}_L^A : \right) + 2\frac{N+1}{N} \mathcal{J}_R^A \mathcal{J}_L^A \\ & - \frac{N^2-1}{N^2} \mathcal{J}_R^0 \mathcal{J}_L^0. \end{aligned} \quad (\text{A16})$$

As a consequence, the continuum limit of the SU(N) Hubbard model at half filling exhibits the spin-charge separation:

$$\mathcal{H} = \mathcal{H}_c + \mathcal{H}_s \quad (\text{A17})$$

with

$$\mathcal{H}_c = \frac{\pi v_c}{N} \left(: \mathcal{J}_R^0 \mathcal{J}_R^0 : + : \mathcal{J}_L^0 \mathcal{J}_L^0 : \right) + G_c \mathcal{J}_R^0 \mathcal{J}_L^0 \quad (\text{A18})$$

and

$$\mathcal{H}_s = \frac{2\pi v_s}{N+1} \left(: \mathcal{J}_R^A \mathcal{J}_R^A : + : \mathcal{J}_L^A \mathcal{J}_L^A : \right) + G_s \mathcal{J}_R^A \mathcal{J}_L^A. \quad (\text{A19})$$

The renormalized velocities are given by:

$$\begin{aligned} v_s & = v_F - \frac{U a_0}{2\pi} \\ v_c & = v_F + (N-1) \frac{U a_0}{2\pi} \end{aligned} \quad (\text{A20})$$

whereas the current-current couplings in the charge and the spin sectors write:

$$\begin{aligned} G_c & = \frac{N-1}{N} U a_0 \\ G_s & = -2U a_0. \end{aligned} \quad (\text{A21})$$

-
- [1] N. F. Mott, *Metal-Insulator Transitions*, Taylor-Francis (1990).
 - [2] F. Gebhard, *The Mott Metal-Insulator Transition*, Springer-Verlag (1997).
 - [3] M. Imada, A. Fujimori, and Y. Tokura, *Rev. Mod. Phys.* **70**, 1039 (1998).
 - [4] A. Georges, G. Kotliar, W. Krauth, and M. J. Rozenberg, *Rev. Mod. Phys.* **68**, 13 (1996).
 - [5] D. Jérôme and H. J. Schulz, *Adv. Phys.* **31**, 299 (1982).
 - [6] S. Tarucha, T. Saku, Y. Tokura, and Y. Hirayama, *Phys. Rev. B* **47**, 4064 (1993).
 - [7] F. D. M. Haldane, *Phys. Rev. Lett.* **45**, 1840 (1981); *J. Phys. C* **14**, 2585 (1981).
 - [8] For recent reviews, see: J. Voit, *Rep. Prog. Phys.* **58**, 977 (1995); H. J. Schulz, G. Cuniberti, and P. Pieri, *cond-mat/9807366*.
 - [9] T. Giamarchi, *Phys. Rev. B* **44**, 2905 (1991); T. Giamarchi and A. J. Millis, *Phys. Rev. B* **46**, 9325 (1992); T. Giamarchi, *Physica B* 230-232, 975 (1997).
 - [10] H. Schulz, in *Strongly Correlated Electronic Materials*, edited by K. S. Bedell et al., 187 Addison-Wesley (1994).
 - [11] E. H. Lieb and F. Y. Wu, *Phys. Rev. Lett.* **20**, 1445 (1968).
 - [12] P. Schlottmann, *Phys. Rev. B* **45**, 5784 (1992) and references therein.
 - [13] H. Frahm and A. Schadschneider, *J. Phys. A: Math. Gen.* **26**, 1463 (1993).
 - [14] E. Dagotto, *Rev. Mod. Phys.* **66**, 763 (1994).
 - [15] Lectures Notes on ‘‘Density-Matrix Renormalization Group’’, Dresden (Germany 1998) I. Peschel, K. Hallberg, and X. Wang (eds.). Springer-Verlag 1999.
 - [16] S. R. White, *Phys. Rev. B* **48**, 10345 (1993).

- [17] S. R. White, Phys. Rep. **301**, 187 (1998).
- [18] W. von der Linden, Phys. Rep. **220**, 53 (1992).
- [19] N. Trivedi and D. M. Ceperley, Phys. Rev. B **41**, 4552 (1990).
- [20] M. Beccaria, C. Presillia, G. Fabrizio De Angelis, and G. Jona-Lasinio, cond-mat/9810347.
- [21] W. Krauth and O. Pluchery, J. Phys. A **27**, L715 (1994).
- [22] W. Krauth and M. Mézard, Z. Phys. B **97**, 127 (1995).
- [23] I. Affleck, Nucl. Phys. **B265**, 409 (1986); I. Affleck and F. D. Haldane, Phys. Rev. B **36**, 5291 (1987); I. Affleck, Nucl. Phys. **B305**, 582 (1988).
- [24] For a review, see for instance: A. M. Tsvelik, *Quantum Field Theory in Condensed Matter Physics*, Cambridge University Press (1995); A. O. Gogolin, A. A. Nersesyan, and A. M. Tsvelik, *Bosonization and Strongly Correlated Systems*, Cambridge University Press (1998).
- [25] B. Sutherland, Phys. Rev. B **12**, 3795 (1975).
- [26] P. Di Francesco, P. Mathieu, and D. Sénéchal, *Conformal Field Theory*, Springer-Verlag (1997).
- [27] H. J. Schulz, Phys. Rev. Lett. **65**, 2462 (1990).
- [28] H. Frahm and V. E. Korepin, Phys. Rev. B **42**, 10 553 (1990).
- [29] N. Kawakami and S. K. Yang, J. Phys.: Condens. Matter **3**, 5983 (1991).
- [30] J. Voit, Phys. Rev. B **45**, 4027 (1992).
- [31] P. Azaria, A. O. Gogolin, P. Lecheminant, and A. A. Nersesyan, preprint (1999).
- [32] C. Itoi and M.-H. Kato, Phys. Rev. B **55**, 8295 (1997).
- [33] H. W. J. Blote, J. L. Cardy, and M. P. Nightingale, Phys. Rev. Lett. **56**, 742 (1986); I. Affleck, Phys. Rev. Lett. **56**, 746 (1986).
- [34] J. Carlson, Phys. Rev. B **40**, 846 (1989).
- [35] M. Gross, E. Sanchez-Velasco, and E. Siggia, Phys. Rev. B **39**, 2484 (1989).
- [36] K. J. Runge, Phys. Rev. B **45**, 7229 (1992).
- [37] M. Ogata and H. Shiba, Phys. Rev. B **41**, 2326 (1990).
- [38] C. J. Umrigar, K. G. Wilson, and J. W. Wilkins, Phys. Rev. Lett. **60**, 1719 (1988).
- [39] B. S. Shastry and B. Sutherland, Phys. Rev. Lett. **65**, 243 (1990).
- [40] R. Assaraf, P. Azaria, M. Caffarel, and P. Lecheminant, in preparation.
- [41] N. Kawakami, Phys. Rev. B **47**, 2928 (1993); T. Fujii, Y. Tsukamoto, and N. Kawakami, cond-mat/9811189.
- [42] M. Oshikawa, M. Yamanaka, and I. Affleck, Phys. Rev. Lett. **78**, 1984 (1997).
- [43] K. Totsuka, Phys. Lett. A **228**, 103 (1997); Phys. Rev. B **57**, 3454 (1998).
- [44] D. C. Cabra, A. Honecker, and P. Pujol, Phys. Rev. Lett. **79**, 5126 (1997); Phys. Rev. B **58**, 6241 (1998).